공학박사 학위논문

# Unconstrained Sleep Monitoring and Modulation using Deep Neural Networks and Closed-Loop Stimulation

심층 신경망 및 폐-루프형 자극을 이용한
무구속적 수면 모니터링 및 조절

2020년 2월

서울대학교 대학원
협동과정 바이오엔지니어링 전공
최 상 호

**Ph.D. Dissertation**

# Unconstrained Sleep Monitoring and Modulation using Deep Neural Networks and Closed-Loop Stimulation

**February 2020**

**Interdisciplinary Program in Bioengineering**
**The Graduate School**
**Seoul National University**

**Sang Ho Choi**

# Abstract

# Unconstrained Sleep Monitoring and Modulation using Deep Neural Networks and Closed-Loop Stimulation

**Sang Ho Choi**
**Interdisciplinary Program in Bioengineering**
**The Graduate School**
**Seoul National University**

Sleep is a natural state of our mind and body that plays an essential role in maintaining our health and enhancing our memory. An effective approach to monitor sleep and promote sleep quality would improve our health and well-being. Though previous studies proposed several methods to achieve this, they are obtrusive and impractical in the real world and are inadequate for long-term use; hence, a new approach is essential. This thesis proposes deep neural networks based sleep stage classification model utilizing an unconstrained ballistocardiography (BCG)

waveform. In addition, it suggests a novel unobtrusive sleep stimulation system and evaluates its effects on sleep and memory.

Sleep stage scoring is the first step in sleep monitoring. Polysomnography (PSG) is the gold standard method for assessing sleep; however, it is obtrusive and difficult to use for long-term sleep monitoring. To overcome these limitations, a LSTM model, for automatic sleep stage scoring using BCG signals measured without constraints is proposed. The BCG signals of 60 participants were recorded using a polyvinylidene fluoride sensor during PSG. Of the 60 recordings, 30 were used for training, 10 for validation, and 20 for testing. Sixteen parameters including movement, respiration and heart rate variability (HRV) were extracted from the BCG signals and then normalized. From the LSTM architecture, four sleep stage classification performances were evaluated for a test dataset, and the results were compared with conventional machine learning results. An epoch-by-epoch (30 s) analysis of the four sleep stages showed an average accuracy of 0.74 and a Cohen's kappa coefficient of 0.55. When compared with other machine learning methods and previous studies, the proposed LSTM model achieved the highest classification performance. The use of LSTM networks with BCG signals has the potential to enable automatic sleep stage scoring and can be used for long-term sleep monitoring at home.

To enhance sleep quality and promote health through sleep, a sleep modulation method that extends beyond passive sleep monitoring is required. Although various stimulation systems for enhancing sleep exist, they are constrained and impractical for long-term use. This thesis overcomes the limitations of other methods by suggesting a new stimulation method and examining the effects of stimulation on the heart rhythm and sleep. The effects of open-loop vibration stimulation during sleep

were assessed by the sleep macrostructure and HRV analysis. Although the sleep onset latency parameter decreased significantly during night sleep, had no effect on the autonomic nervous system (ANS) stabilization. To increase the interaction between the heart rhythm and the vibration stimulus, a novel closed-loop stimulation system was developed and confirmed its feasibility of application for sleep. Ten volunteers participated in the evaluation experiment, in which they took a nap for approximately 90 min. The experiment comprised one baseline and three stimulation conditions. From the HRV and heart rate density analysis, the closed-loop stimulation method influenced the heart rhythm and stabilized the ANS. A small detuning percent modulated the heart rhythm more effectively. When comparing the effects of sleep stimulation methods such as auditory, current, and vibration, the proposed closed-loop stimulation system was most effective in modulating the heart rhythm. In HRV analysis, only the closed-loop stimulation method stabilized the ANS. Therefore, this system could be an innovative method for applying external stimulation during sleep.

To examine the effects of an external periodic stimulus on sleep and memory, closed-loop vibration stimulation was induced for the whole night's sleep. Twelve volunteers participated in the experiment and each underwent one adaptation night and two experimental conditions such as a stimulation condition (STIM) and a no stimulation condition (SHAM). The effect of the developed system on memory was assessed using a word pair associated learning task. The HRV analysis showed a significant increase in the parasympathetic activity, and the sympathovagal balance significantly decreased under the STIM condition during the N3 sleep stage. The synchronization ratio between the heartbeat and the stimulus significantly increased

under the STIM condition in the N3 stage. The electroencephalogram (EEG) spectral analysis showed an enhanced EEG spectral power of slow-wave activity and theta frequency bands, during the STIM condition in the N3 stage. Memory retention significantly increased under the STIM condition compared with the SHAM condition. These findings suggest that closed-loop stimulation improves the N3 stage's quality and memory retention. This method has a positive effect on the ANS and neural function during sleep.

The proposed unconstrained sleep stage classification method would contribute to monitoring sleep long-term. Furthermore, the proposed new stimulation method would enhance sleep quality and has the potential to enhance health through sleep modulation. The approaches are expected to open a new strategy for monitoring and enhancing sleep in a convenient and safe manner.

**Keyword : unconstrained, sleep monitoring, long short-term memory networks, sleep modulation, closed-loop system, sleep medicine.**

**Student Number : 2014-21547**

# Table of Contents

# List of Tables

# List of Figures

# List of Abbreviations

| | |
|---|---|
| **AASM** | American academy of sleep medicine |
| **ACT** | Actigraphy |
| **ANS** | Autonomic nervous system |
| **BCG** | Ballistocardiography |
| **BP** | Blood pressure |
| **BPM** | Beats per minute |
| **CNN** | Convolutional neural network |
| **DA** | Discriminant analysis |
| **DT** | Decision trees |
| **ECG** | Electrocardiogram |
| **EEG** | Electroencephalogram |
| **EMG** | Electromyogram |
| **EOG** | Electrooculogram |
| **FC** | Fully connected |
| **FFT** | Fast Fourier transform |
| **FIR** | Finite impulse response |
| **HF** | High-frequency |
| **HR** | Heart rate |
| **HRV** | Heart rate variability |
| **KAPPA** | Cohen’s kappa coefficient value |
| **kNN** | k-nearest neighbor |
| **LF** | Low-frequency |

| | |
|---|---|
| **LF/HF** | The ratio of the LF power to the HF power |
| **LSTM** | Long short-term memory |
| **mHR** | Mean of HR |
| **NN** | Normal-to-normal |
| **NREM** | Non-rapid eye movement |
| **PAT** | Peripheral arterial tonometry |
| **pNN50** | Percentage of successive NN intervals that differ by more than 50 |
| **PO** | Pulse oximetry |
| **PPG** | Photoplethysmogram |
| **PSG** | Polysomnography |
| **PVDF** | Polyvinylidence fluoride |
| **R&K** | Rechtschaffen & kales |
| **REM** | Rapid eye movement |
| **RF** | Random forests |
| **RIP** | Respiratory inductance plethysmography |
| **RMSSD** | Root mean square of successive NN-interval differences |
| **RNNs** | Recurrent neural networks |
| **RSA** | Respiratory sinus arrhythmia |
| **SD** | Standard deviation |
| **SDNN** | Standard deviation of the NN intervals |
| **SFI** | Sleep fragmentation index |
| **SHAM** | No stimulation condition |
| **SOL** | Sleep onset latency |
| **STIM** | Stimulation condition |

| | |
|---|---|
| **SVM** | Support vector machine |
| **SWA** | Slow wave activity |
| **SWS** | Slow wave sleep |
| **TRT** | Total recording time |
| **TST** | Total sleep time |
| **WASO** | Wake after sleep onset |

# 1
# Introduction

## 1.1. Sleep Functions and Architecture

Humans sleep almost one-third of their lifetimes. Sleep plays an important role in our lives in terms of health and well-being. The primary role of sleep is to save energy, restore physical and cognitive performance, and improve mood [1]–[6]. Sleep enhances creativity, including cognitive flexibility [7], [8], and plays a major role in promoting brain plasticity, synaptic reconstruction, and learning [3], [9]–[11]. In contrast, sleep deprivation and sleep disorders negatively influence mood [12], cognitive performance, and motor function [13], [14] and increase the risk of cardiovascular diseases [15]–[17] and obesity [18], [19]. In addition, a lack of sleep can interfere with work, family, and social life. Thus, monitoring sleep and enhancing its quality are significant for a healthy life.

Wakefulness and sleep are associated with physiological states change. Normal human sleep stage scoring rules were first defined by Rechtschaffen & Kales (R&K) in 1968 [20] and adapted by the American Academy of Sleep Medicine (AASM) [21]. Sleep stages are scored by different characteristics of electroencephalogram

(EEG), electrooculogram (EOG), and electromyogram (EMG) and sleep comprises two states: rapid eye movement (REM) sleep and non-rapid eye movement (NREM) sleep. NREM and REM sleep alternate through the night at about 90-minutes (approximately 4-6 NREM-REM cycles during night sleep). According to the AASM manual, NREM sleep is further divided into N1, N2, and N3 sleep stages (Figure 1-1(a)). N1 sleep stage (2-5% of sleep time) is the lightest sleep stage and is a transition state from wakefulness to sleep. It is defined by attenuated EEG alpha rhythm (8–13 Hz) and the appearance of low-amplitude mixed-frequency EEG activity. N2 sleep stage (45-55% of sleep time) is characterized by the appearance of sleep spindle and K-complex. Sleep spindle is a train of distinct sinusoidal waves with frequency 11–16 Hz lasting at least 0.5 s. K-complex is a negative sharp wave followed by a positive wave lasting more than 0.5 s. N1 and N2 sleep stages are called as light sleep. N3 sleep stage (13-23% of sleep time) is the deepest sleep stage and is called deep sleep or slow wave sleep (SWS). It is defined by high amplitude slow wave activity (SWA, 0.5–4 Hz) accounting for more than 20% of an epoch (30 s). REM sleep stage (20-25% of sleep time) is associated with REM in the EOG, low-amplitude and mixed-frequency EEG, and low chin EMG tone. The distribution of each sleep stage across a sleep period is called as sleep architecture and it is visualized in the form of a hypnogram (Figure 1-1(b)).

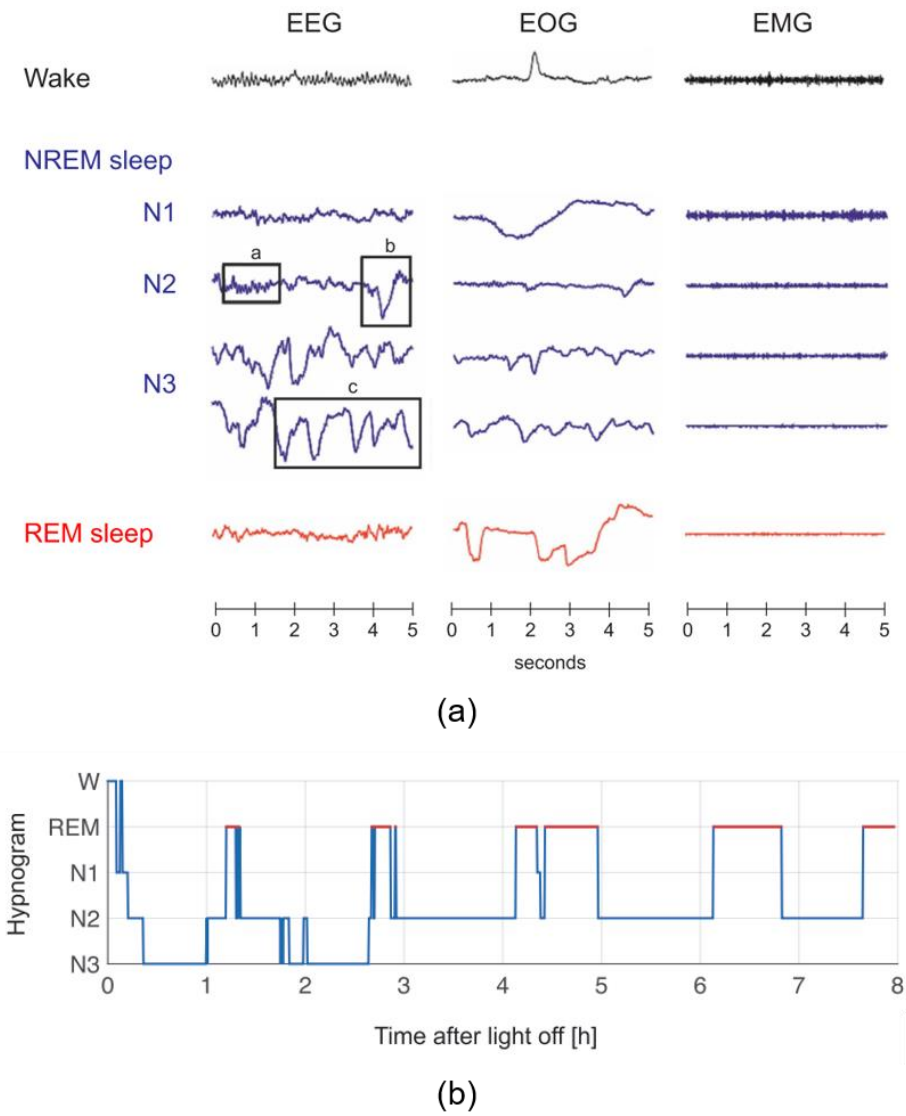


**Figure 1-1.** (a) EEG, EOG, and EMG signals during wake and each sleep stage. a: Sleep spindle, b: K-complex, c: Slow oscillation, (b) Hypnogram with sleep stages (W: wakefulness, REM: REM sleep, N1-N3: NREM sleep stages). (*Source*: [22])

## 1.2. Sleep Monitoring

Polysomnography (PSG) is the gold standard method to determine sleep stages. PSG records multichannel biomedical signals such as EEG, EOG, EMG, electrocardiogram (ECG), and other signals. According to the manual of the AASM [21], sleep experts visually score sleep stages every 30 s into wake, NREM stages 1–3, and REM sleep. Although PSG has been used to assess sleep, there are many limitations: (1) As shown in Figure 1-2, numerous sensors are attached to the body and it is uncomfortable and thus, long-term monitoring is difficult. Further, the inconvenience caused by the sensors may disturb normal sleep. (2) A sleep expert who can conduct PSG based on AASM manual is necessary; in addition, conducting PSG and the sleep stage scoring process are labor-intensive and time-consuming tasks. (3) Because sleep experts score sleep stages visually, it is subjective and may have human errors. Several studies have reported that manual scoring of sleep stages by sleep experts exhibit inter-rater variability [23]–[25].

To overcome these limitations, several smart devices have been commercialized to monitor sleep with the usual home environments [26]. Movement-based sleep monitoring, such as Actigraphy (ACT) [11], [27], mobile, and wearable devices [28]–[30] has become the easiest and most used method. In addition, some methods involve the installation of devices in sleeping environments without attaching sensors to the user, for example, bed ACT [31], the use of polyvinylidence fluoride (PVDF) film sensors [32], Doppler radar [33], [34], and near-infrared videos [35], [36].

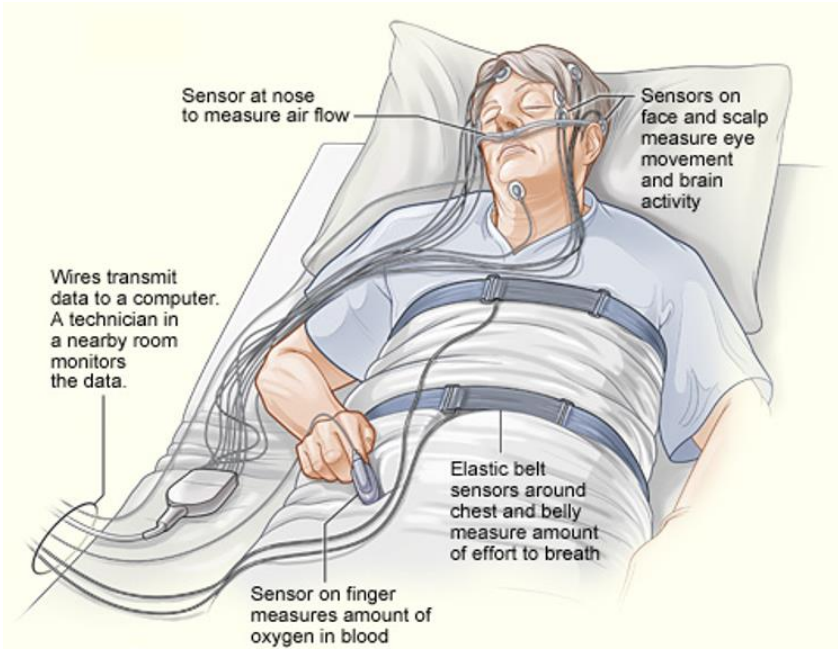


**Figure 1-2.** Sensors for standard polysomnography.
(*Source*: National Heart Lung and Blood Institute)

Furthermore, many studies have attempted to classify sleep stages automatically using the minimum number of signals [26]. In a previous study [37], [38], a single channel EEG measured during PSG was used to score sleep stages. Wrist activity was used to develop and evaluate automatic sleep scoring methods [27], [39]. The variation of autonomic nervous system (ANS) has been studied, and it was found that it is associated with sleep stages [40]–[44]. With the progression of the sleep stage from N1 to N3, sympathetic activity decreases and parasympathetic activity increases. In contrast, during REM sleep, sympathetic activity is more dominant and becomes unstable like in wakefulness. From these characteristics, heart rate variability (HRV) parameters that represent ANS activity have been considered one of the most useful features for sleep staging. The HRV parameters derived from ECG signals were used for automatic sleep scoring [45]–[48].

Peripheral arterial tonometry (PAT) signal, which indicates peripheral vasoconstriction, was recorded with an ambulatory wrist-worn device and used to estimate sleep stages [49]–[51]. Photoplethysmogram (PPG)-based sleep stage classification was also studied [52]. Although these studies developed an automatic sleep stage scoring method using the minimum number of signals, it is still inconvenient for the user to attach sensors during sleep, thereby decreasing their applicability for long-term monitoring.

Recently, deep learning [53], a branch of machine learning methods that comprises multiple layers to learn and extract representation features from input data, has been used in object detection, speech recognition, visual recognition, and many other fields. Deep learning has brought breakthroughs in many fields, and it has also been applied to automatic sleep stage classification studies. Phan *et al*. [54] introduced a joint classification and prediction multi-task convolutional neural network (CNN) framework for automatic sleep stage classification using EEG, EOG, and EMG signals. Stephansen *et al*. [55] used a large dataset comprising 3,000 normal and abnormal sleep recordings and proposed a CNN+Long Short-Term Memory (LSTM) model with EEG, EOG, and EMG signals for automatic sleep stage scoring. These studies achieved a high sleep stage classification performance; however, they required multiple signal modalities. To minimize the number of signals used, several studies have developed a deep learning-based sleep stage estimation model using only one channel EEG [37], [56], [57]. Although the sleep stage can be estimated by applying a deep learning method from a one-channel EEG signal, the sensor should be attached to the body to measure the EEG signal, which is inconvenient for the user and impractical for long-term sleep monitoring.

## 1.3. Sleep Modulation

Several smart technologies have been developed to monitor sleep in the typical home environment [26]. However, although such methods provide the user with sleep information, a method that extends beyond the passive monitoring of sleep is required to enhance sleep quality and promote health levels through sleep. To enhance sleep, soothing sounds or music and feet warming are commonly used among the general population [58], [59]. In addition, rocking movements appear to help people relax or fall asleep. Swinging a baby in a hammock or physical rocking movements can be helpful in inducing sleep and appear to be effective for adults as well [60]–[63].

Several methods have been developed to increase sleep efficacy by enhancing the SWA. SWA, which represents the EEG spectral power in the 0.5–4 Hz band during NREM sleep, is an important contributor to memory consolidation and brain restoration [64]. Intermittent transcranial direct-current stimulation increases SWS and the <1 Hz slow oscillation during stimulation-free intervals [65]. Another study demonstrated that slow waves can be triggered in sleeping subjects with transcranial magnetic stimulation [9]. An auditory stimulation method has been shown to enhance slow oscillation [66]. Recently, many studies that use these methods to enhance brain oscillations and improve sleep and memory consolidation have been conducted [10], [67]–[70]. However, although these methods affect sleep, their safety is questionable, and they are considered impractical for long-term use. Thus, other stimulation systems for enhancing sleep quality are needed.

In many natural phenomena, oscillating objects with their own rhythm interact with the environment [71]; e.g., thousands of fireflies blinking on and off in unison.

Fireflies interact with other insects via light pulses, and each firefly is affected by the light created by the entire population [72]. A cricket's chirps are influenced by the chirps of its neighbors. A cricket responds to the preceding chirp and achieves synchrony by either lengthening or shortening its chirp [73]. Moreover, interactions are also present in human physiological systems; there are interactions in human internal subsystems such as respiratory sinus arrhythmia (RSA), which refers to the periodic variation in the heart rate (HR) according to the respiratory cycle [74]. In addition, the cardiac system interacts with brain activity [75], [76] and locomotor rhythms [77], [78].

Furthermore, the internal physiological system is influenced by environmental conditions and change. The circadian rhythm represents the behavior of humans by a 24 h cycle of sleep and wakefulness. This cycle is entrained by the daily cycle of light and dark [79], [80]. McClintock reported that social interaction influences some aspects of the menstrual cycle [81]. Van Leeuwen *et al*. [82] verified phase synchronization, which implies the existence of phase locking between two weakly interacting systems, such as between the fetal and the maternal HRs, even though they are ANS with separate blood circulation. They stated that maternal-fetal heart coupling is mediated by the acoustic stimulation of maternal heartbeat and vascular pulsations, which are recognized by the fetal auditory system. These stimuli can act on external forced rhythms to accompany the heartbeat of the fetus with that of the mother. Grimaldi *et al*. [83] were the first to prove that acoustic enhancement of SWA during sleep enhances parasympathetic activity. They stated that acoustic stimulation strengthened the coupling between cortical and cardiac oscillations, reflected in the concomitant changes in SWA and HRV. A study, which assessed the

interaction between an internal physiological system and external forces, showed that the HR can be entrained through a weak external noninvasive force in the form of visual and auditory stimuli [84]. Yoon *et al*. [85] found experimental evidence that couples' cardiac rhythms influence each other during co-sleeping. This finding may be attributed to weak cardiac vibrations that are transmitted from one individual to another through a mechanical bed connection. These studies showed that the intrinsic physiological rhythm could be entrained and interact with the periodic rhythm of other systems in at least one neural, mechanical, or behavioral connection.

## 1.4. Motivation and Objectives

For long-term monitoring of sleep in a residential environment, it is essential that physiological signals are measured in an unconstrained and unobtrusive manner during sleep. Ballistocardiography (BCG) is an unobtrusive method measuring the recoil force of the body when subtle body movement generated by the heart ejects blood into the arteries [86]. Because BCG is a noninvasive method, it can be measured without disturbing human sleep for an extended period. Furthermore, LSTM networks that have advantages of being able to learn long-term dependencies were employed to automatically learn temporally sequential patterns. The sleep expert classifies the current sleep epoch from a sequence of previous epoch information, and therefore, the LSTM is a suitable deep learning model that it could automatically learn a conventional scoring strategy in sleep clinics. In this thesis, the sleep stages classification LSTM model was developed using unconstrainedly measured BCG signal during sleep, and the performance was compared with other machine learning methods and previous works.

To enhance sleep quality and promote health levels through sleep, there needs a sleep modulation method that extends beyond passive sleep monitoring. Human intrinsic physiological rhythm could be entrained and interact with the periodic rhythm of other systems in at least one neural, mechanical, or behavioral connection. From this point of view, an external weak vibration stimulus could influence heart rhythm and stabilize the ANS during sleep. Furthermore, if detuning, which represents the frequency difference between an oscillator and an external force, is small, even a very small force can entrain the oscillator [71]. Thus, it was hypothesized that a smaller amount of detuning is appropriate for modulating heart rhythm. In this thesis, a novel closed-loop vibration stimulation system, which stimuli were induced by an unconstrained manner, was developed and investigated the effect of stimulation on heart rhythm during naps. In addition, effects on heart rhythm according to stimulation methods were compared. Then the developed stimulation system was applied during night sleep with the PSG test and analyzed sleep modulation effects.

## 1.5. Outline of the Thesis

This thesis consists of following chapters.

- Chapter 2 presents the deep neural networks approach for unconstrained sleep monitoring using BCG signals and discusses the potential applicability of the model compared with other methods.
- Chapter 3 describes the effects of stimulation methods on heart rhythm during sleep. Specifically, this chapter presents the closed-loop stimulation system for unconstrained sleep modulation, assesses the effects on heart

rhythm during naps, and discusses its applicability to sleep.

- Chapter 4 deals with the effects of the developed stimulation system on night sleep in macrostructure and microstructure perspective. In addition, the effects of stimulation on memory are assessed.
- Chapter 5 summarizes the conclusions of the preceding chapters.

This thesis is based on following scientific articles that have been published (chapter 3), submitted for publication (chapter 2), and is in the final preparation steps for manuscript submission (chapter 4):

- Chapter 2

  S. H. Choi, *et al*., "Long Short-Term Memory Networks for Unconstrained Sleep Stage Classification by Ballistocardiography," *IEEE JBHI*, under review.
- Chapter 3

  S. H. Choi, *et al*., "Effect of Closed-Loop Vibration Stimulation on Heart Rhythm during Naps," *Sensors*, 19(19), 4136, 2019.
- Chapter 4

  S. H. Choi, *et al*., "Closed-Loop Vibration Stimulation during Sleep Improves Declarative Memory," in preparation.

The author of this thesis contributed to the above studies as follows: conception and design of the experiments; developed the device; data acquisition, analysis, and interpretations; and wrote and reviewed the manuscript.

# 2

# Deep Neural Networks for Unconstrained Sleep Stage Classification by Ballistocardiography

An unconstrained sleep monitoring method is investigated in this chapter. Based on unconstrainedly measured BCG signal, LSTM network model is proposed for classifying sleep stage automatically. An optimal LSTM architecture that produces the best performance is searched. Sleep stage classification performance of the LSTM model is compared with other machine learning methods. In addition, the classification performance is also evaluated with previous works and the application will be discussed.

## 2.1. Methods

### 2.1.1. PSG Data and BCG Acquisition

The Institutional Review Board of Seoul National University Hospital approved the retrospective study (IRB No. C-1906-131-1042). The dataset consists of PSG recordings and BCG signals recorded from participants overnight at the Center for

Sleep and Chronobiology, Seoul National University Hospital. Participants who were 18–60 years of age and had no symptoms related to sleep were included. The exclusion criteria for this study were as follows: people with (1) a history of severe physical or psychological illnesses, (2) unstable vital signs, (3) arrhythmia, (4) sleep disorders (e.g., periodic limb movement disorder, restless legs syndrome, sleepwalking, sleep terrors, obstructive sleep apnea, and REM sleep behavior disorders). Sixty PSG recordings that satisfied the inclusion and exclusion criteria were used in this study. Table 2-1 summarizes the sleep-related variables and demographics of the participants.

Overnight PSG data were recorded using a standard PSG routine [21]: EEG electrodes at positions F3, F4, C3, C4, O1, and O2, and EMG from the chin and bilateral tibialis anterior muscles, ECG at lead II, bilateral EOGs, oronasal airflow, nasal pressure, thoracic and abdominal respiration, and blood oxygen saturation. The sleep stages were scored by sleep technologists and verified by a sleep clinician according to the 2012 AASM manual [21]. The scored sleep stages were used as reference classes when training LSTM networks.

A very thin and flexible PVDF was used as a sensor for measuring several physiological signals such as respiration [87], [88], HR [89], and BCG [90], [91]. The BCG signals were measured using the PVDF sensor at a 250-Hz sampling rate. To avoid direct contact with the body of the participant, the PVDF sensor was installed between the mattress and the mattress cover. Furthermore, the sensor was positioned near the heart of the participant when he/she was lying on the bed. The PVDF sensor was thin enough for the BCG signals to be measured from the participant in an unconstrained and unobtrusive manner.

**Table 2-1.** Summary of sleep-related variables and demographics

| Variables | Mean ± S.D. |
|---|---|
| Gender (male/female) | 34/26 |
| Age (years) | 29.2 ± 9.7 |
| BMI (kg/m$^2$) | 22.0 ± 3.6 |
| AHI (events/h) | 2.2 ± 3.6 |
| Total recording time (min) | 450.3 ± 39.0 |
| Total sleep time (min) | 408.4 ± 47.9 |
| Sleep efficiency (%) | 90.7 ± 6.9 |
| Stage wake (%) | 9.3 ± 6.9 |
| Stage N1 & N2 (%) | 62.6 ± 9.4 |
| Stage N3 (%) | 9.0 ± 7.0 |
| Stage REM (%) | 19.1 ± 5.9 |

S.D., standard deviation; BMI, body mass index; N, non-rapid eye movement; REM, rapid eye movement; AHI, apnea hypopnea index.

### 2.1.2. Parameter Extraction

Many studies [40]–[43] have confirmed that there is a high correlation between sleep stage variation and ANS activation. As sleep deepens from wakefulness to deep sleep stage, heart rate and sympathetic tone are significantly decreased and parasympathetic tone is significantly increased. While under REM sleep, these values return to levels similar to that of the wake stage. Owing to the ANS effect, respiratory rhythm is characterized by a slower and more regular rhythm as the sleep becomes deeper during NREM sleep. Wakefulness and REM sleep are also characterized with disturbed respiratory dynamics. Furthermore, physical movement is one of the dominant parameters to separate wakefulness and sleep.

Based on above physiological characteristics during wakefulness and sleep, sixteen parameters were extracted from the BCG signal. The descriptions of the extracted parameters are listed in Table 2-2. A movement parameter (mov) was obtained by processing the BCG signals with high-pass (2 Hz) and low-pass (15 Hz) fifth-order IIR Butterworth filters. Then, the square root of the average of the squared data from the absolute value of the filtered signal is extracted every 30 s. To extract

respiration related parameters, the RSA signal was extracted by filtering the BCG signal with a high-pass (0.15 Hz) and low-pass (0.4 Hz) fifth-order IIR Butterworth filter. Then, the respiration frequency (fRSA) parameter was obtained from the RSA signal using an autocorrelation method [92] at intervals of 30 s.

J-peak was detected as follows. First, the BCG signal was filtered within a range of 2–15 Hz (5th-order Butterworth filter, IIR) to extract clear heartbeat derived signals. Subsequently, the absolute values of the filtered signals were acquired to obtain positive peaks. Then, a moving average filter was applied to smooth out the peaks and a 0.5 Hz high-pass filter was applied to remove baseline drift. Finally, J-peak was detected using the findpeaks function of MATLAB, which finds the values and locations of local maxima in signal data. After detecting J-peak, post-processing was conducted to remove artifacts. When the position of the peak in the autocorrelation was in the predetermined range of 0.5–1.7 s lag for HR, this position was considered normal. If there was no peak in the range, it was determined to comprise artifacts. The J-peak positions in the artifacts and movement sections were considered as errors and canceled. The mean heart rate (mHR) was calculated every 30 s from the BCG consecutive J-peak intervals (JJI), and the frequency-domain HRV parameters were calculated every 5 min. The JJI were interpolated with a shape-preserving precise cubic method. Then, the spectral power of JJI in the low-frequency range (0.04–0.15 Hz) and high-frequency range (0.15–0.4 Hz) were extracted using a fast Fourier transform (FFT) method. The standard deviation of fRSA (tfRSA) and mHR (tmHR) were calculated every 10 epochs with a sliding window of 1 epoch. To attenuate the noise and reflect a long-term trend, a Savitzky–Golay finite impulse response (FIR) smoothing filter [93] was applied with a

polynomial order of 2 and window size of 31 epochs; then smoothed parameters were extracted as listed in Table 2-2. After extracting 16 parameters, each parameter was normalized using the z-score method which subtracts their average and divides it by their standard deviation (SD) to reduce inter-participant variability.

**Table 2-2.** Descriptions of extracted 16 parameters associated with movement, respiration, and HRV

| Association | Parameter | Description |
|---|---|---|
| Movement | mov | Magnitude of movement from filtered BCG signals |
| Respiration | $f_{RSA}$ | Respiratory frequency derived from BCG signals |
| | $tf_{RSA}$ | Standard deviation of $f_{RSA}$ |
| | $sf_{RSA}$ | Smoothed value of $f_{RSA}$ |
| | $stf_{RSA}$ | Smoothed value of $tf_{RSA}$ |
| | $sdf_{RSA}$ | Smoothed value of absolute difference between $f_{RSA}$ and $sf_{RSA}$ |
| Heart rate variability | mHR | Mean of HR |
| | LF | Spectral power of JJI in low-frequency range (0.04–0.15 Hz) |
| | HF | Spectral power of JJI in high-frequency range (0.15–0.4 Hz) |
| | LFHF | LF to HF ratio |
| | tmHR | Standard deviation of mHR |
| | smHR | Smoothed value of mHR |
| | stmHR | Smoothed value of tmHR |
| | sdmHR | Smoothed value of absolute difference between mHR and smHR |
| | sHF | Smoothed value of HF |
| | sLFHF | Smoothed value of LFHF |

### 2.1.3. LSTM Networks Architecture

Recurrent neural networks (RNNs) are networks with loop-chained structure, which consider temporal series data. RNNs have demonstrated better performance than other machine learning methods for processing sequential inputs such as speech, language, and time series bio-signals [53]. In particular, most successful RNNs are LSTM networks that use a special hidden unit, which is the so-called memory cell. LSTM networks are designed to prevent the vanishing gradient problem that make RNNs difficult to learn to connect information as the length of dependency increases. The core idea behind an LSTM is that the cell state removes or adds information through a forget gate ($f_t$), an input gate ($i_t$), and an output gate ($o_t$) (see Figure 2-1(a)). The following equations represent each process where $\sigma, W, x, b, C, h$ are the sigmoid, weight matrices, input, bias, cell state, and hidden state, respectively.

$$f_t = \sigma(W_f \cdot [h_{t-1}, x_t] + b_f) \tag{2-1}$$

$$i_t = \sigma(W_i \cdot [h_{t-1}, x_t] + b_i) \tag{2-2}$$

$$o_t = \sigma(W_o \cdot [h_{t-1}, x_t] + b_o) \tag{2-3}$$

$$\tilde{C}_t = tanh(W_c \cdot [h_{t-1}, x_t] + b_c) \tag{2-4}$$

$$C_t = f_t * C_{t-1} + i_t * \tilde{C}_t \tag{2-5}$$

$$h_t = \tanh(C_t) * o_t \tag{2-6}$$

Figure 2(b) represents the sleep stage classification process and the selected LSTM architecture comprising two bi-directional LSTM layers, and one fully connected (FC) layer. The LSTM layer comprised 512 units per layer, 16 input dimensions, and 9 sequence lengths that imply 16 extracted parameters and 9 epochs

(270 s) used as an input data segment. From the LSTM layer, 512 output units are connected to a FC layer which classifies the four outputs (WAKE, LIGHT SLEEP: N1+N2, DEEP SLEEP: N3, and REM SLEEP).

Several LSTM structures were trained and validated to optimize hyperparameters in predetermined ranges. An optimal combination of hyperparmeters that produced the best performance in the validation dataset was searched where the candidate of the hyperparameters were as follows: number of LSTM layers {1, 2, 3}; number of LSTM units {16, 32, 64, 128, 256, 512}; lengths of input sequence {1–15}; and type of LSTM structure {unidirectional, bidirectional}. To prevent the model from overfitting, a dropout [94] which is considered an efficient regularization method was used. The value of the dropout was set to 0.25, which means 25% of the units are randomly dropped during each training epoch. Tanh and softmax were used as an activation function for LSTM and the dense layer, respectively. The recurrent activation function of the LSTM was a sigmoid function. The model was trained by using the Adam optimizer [95], and categorical cross-entropy as a loss function. The batch size, learning rate, and the number of training epochs were set to 32, 0.0001, and 50, respectively. The number of training epochs defines the number times that the learning algorithm will work through the entire training dataset.

The structure of LSTM networks was encoded in the name l<ln>_u<un>_s<sn>_<uni/bi>: <ln>, <un>, and <sn> represents the number of LSTM layer, the number of LSTM units, and lengths of input sequence, respectively. <uni/bi> specifies the type of LSTM structure representing “unidirectional” and “bidirectional,” respectively. For example, l2_u512_s9_bi means 2 LSTM layers,

512 units in each layer, an input sequence length of 9 epochs, and a bidirectional LSTM structure.

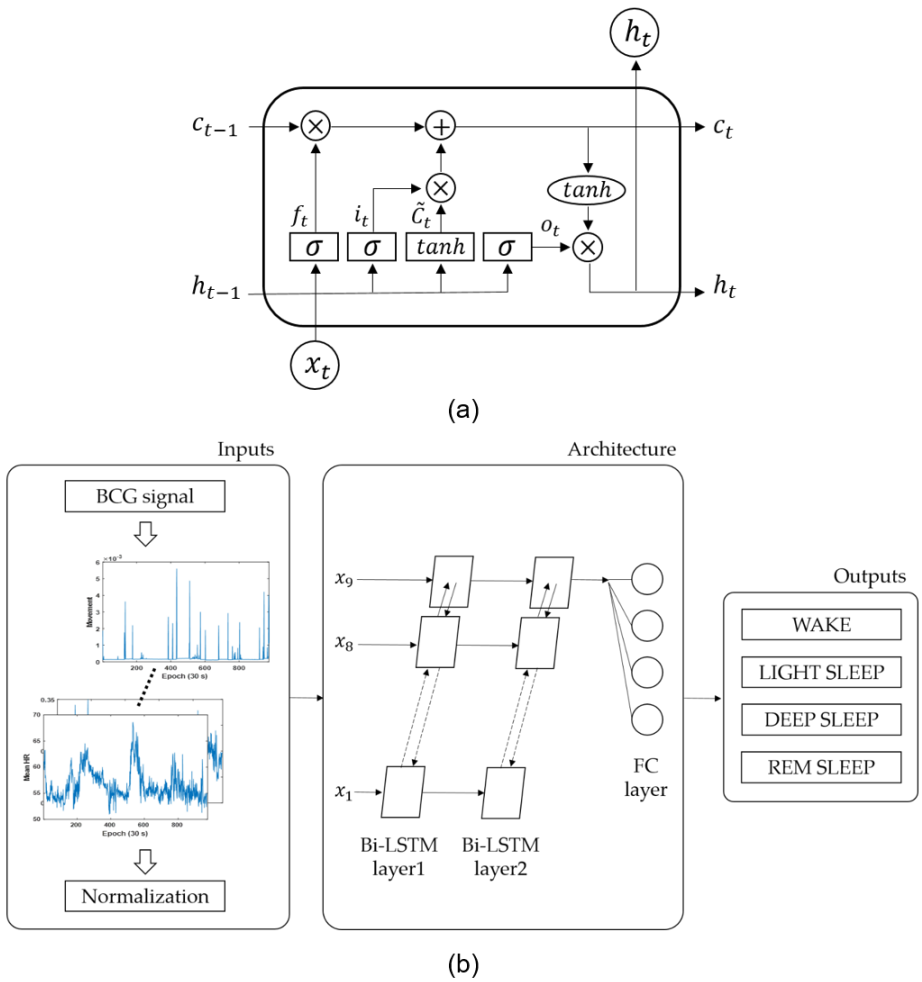


**Figure 2-1.** (a) Unit structure of LSTM (b) LSTM-based sleep stages classification process. LSTM, long short-term memory; Bi-LSTM, bidirectional-LSTM; FC layer, fully connected layer.

### 2.1.4. Training, Validation, and Testing

LSTM networks were trained and validated using a hold-out method for developing a generalized model. In addition, the number of input segments was sufficient for model training. Of the 60 BCG recordings, 30 recordings were used as a training dataset, 10 recordings were used as a validation dataset, and the remaining 20 recordings were used for a testing dataset. Each dataset consisted of randomly selecting BCG recordings. When training the LSTM model, there was a class imbalance problem. For example, the total segments number of the training dataset was 27672 in the selected model, and the numbers of each class segment were 3053, 17135, 2521, and 4963 for wake, light sleep, deep sleep, and REM sleep, respectively. A balance between the number of class segments is necessary to prevent the LSTM model from overfitting to the majority class of Light sleep. There are several methods to balance the number of class segments such as oversampling, undersampling, and assigning different weights. In this study, the previous study method was applied [96], which assigns different weight to each class. In this way, all classes contributed equally to the loss function, just as all classes have the same number of segments when training the model. The weight of class A was computed using the following equation:

$$\text{Class A weight} = \frac{total\ number\ of\ segments}{(number\ of\ classes \times number\ of\ class\ A\ segments)} \tag{2-7}$$

Using this method, all classes contributed equally to the loss function when training the LSTM model and had the effect of preventing overfitting for the majority of classes. In addition, an early stopping method was used to stop the training process

when the validation loss did not improve. During the 50 training epochs, if the validation loss did not decrease for 5 epochs, the training was stopped, and the model weights were reverted to the value that showed the lowest validation loss.

For model implementation, Python 2.7 and the Keras library [97] with Tensorflow as the backend [98] were used. The training and testing were conducted on a workstation with a 3.4 GHz Intel i7-6700 CPU and a GTX1080 8 GB GPU.

| True class \ Predicted class | W | L | D | R |
|---|---|---|---|---|
| W | $TP_W$ | $E_{WL}$ | $E_{WD}$ | $E_{WR}$ |
| L | $E_{LW}$ | $TP_L$ | $E_{LD}$ | $E_{LR}$ |
| D | $E_{DW}$ | $E_{DL}$ | $TP_D$ | $E_{DR}$ |
| R | $E_{RW}$ | $E_{RL}$ | $E_{RD}$ | $TP_R$ |

**Figure 2-2.** Confusion matrix for computing four sleep stage classification performance. TP, true positive; E, error; W, wake; L, light sleep; D, deep sleep; R, rem sleep.

### 2.1.5. Performance Evaluation

To evaluate the sleep stage classification performance, the accuracy and Cohen's kappa coefficient value (KAPPA) [99] were computed, which is used to measure the inter-rater agreement. The equations of the evaluation measures are expressed as follow and $P_e$ is the hypothetical probability of chance agreement:

$$\text{KAPPA} = \frac{P_o - P_e}{1 - P_e} \tag{2-8}$$

$$P_o \text{ (accuracy)} = \frac{\text{TP}_\text{W} + \text{TP}_\text{L} + \text{TP}_\text{D} + \text{TP}_\text{R}}{\text{Total}} \tag{2-9}$$

$$P_e = \sum_{\text{class}=\{\text{W, L, D, R}\}} \frac{\text{TP}_\text{class} + \text{FP}_\text{class}}{\text{Total}} \times \frac{\text{TP}_\text{class} + \text{FN}_\text{class}}{\text{Total}} \tag{2-10}$$

The four sleep stages classification performance was computed using Equations (2-8)–(2-10). During the performance calculation for each sleep stage, the confusion matrix (Figure 2-2) and class of the equation were reduced to 2×2 and two classes, respectively. The LSTM model that showed the highest kappa value in the validation dataset was selected. When the performance of one hyperparameter combination is the same as the other, a low complexity model was selected. Then, the performance of the selected model in the test dataset was evaluated. To obtain objective results, the LSTM model was compared with seven machine learning classifiers, including k-nearest neighbor (kNN) [100], support vector machine (SVM) [101] using linear and rbf kernel, discriminant analysis (DA) [102] using linear and quadratic kernel, decision trees (DT) [103], and random forests (RF) [104]. Regularization and gamma hyperparameters were optimized in SVM models. In addition, max depth of DT and RF models was optimized. The performance of each sleep stage and total sleep stage

classification according to the classifier methods was compared. All classifiers used the same parameters and were implemented using the Scikit-learn library [105].

## 2.2. Results

### 2.2.1. LSTM Networks Performance

To select the optimal combination of hyperparmeters, the performance of the LSTM model was compared in the validation dataset that consisted of 10 recordings. Figure 2-3 presents the sleep stage classification performances in the validation set as changing LSTM model hyperparmeters. Regardless of the LSTM structure (unidirectional and bidirectional) or the number of layers, the classification performance showed an increasing trend as the number of units or sequence length increased. Then each LSTM model was selected that showed the highest performance in the number of layers and structure; Figure 2-4 displays the learning curve of these models on the training and validation datasets. The best performance model that produces the highest KAPPA value in the validation dataset was selected, and the l2_u512_t9_bi LSTM model showed the highest performance.

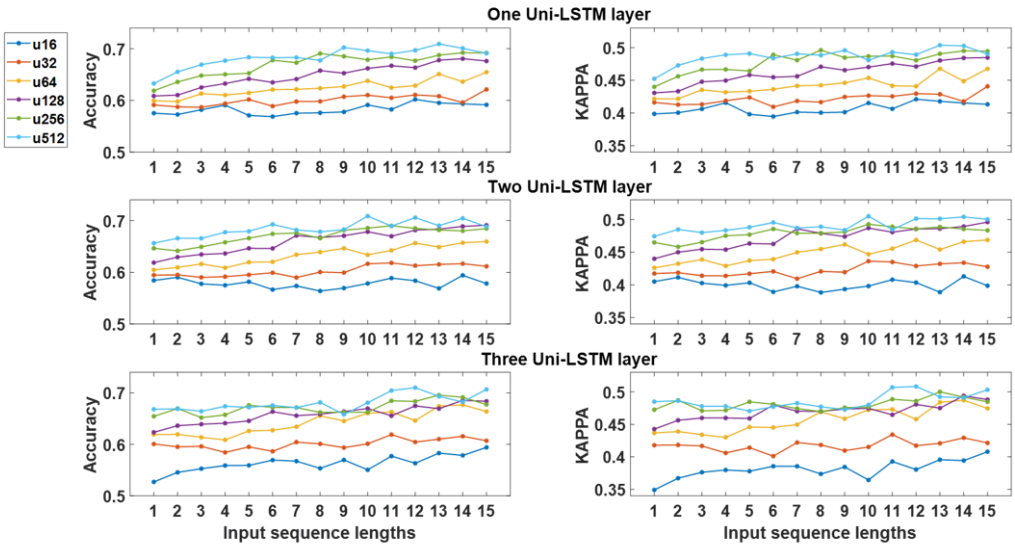


(a)

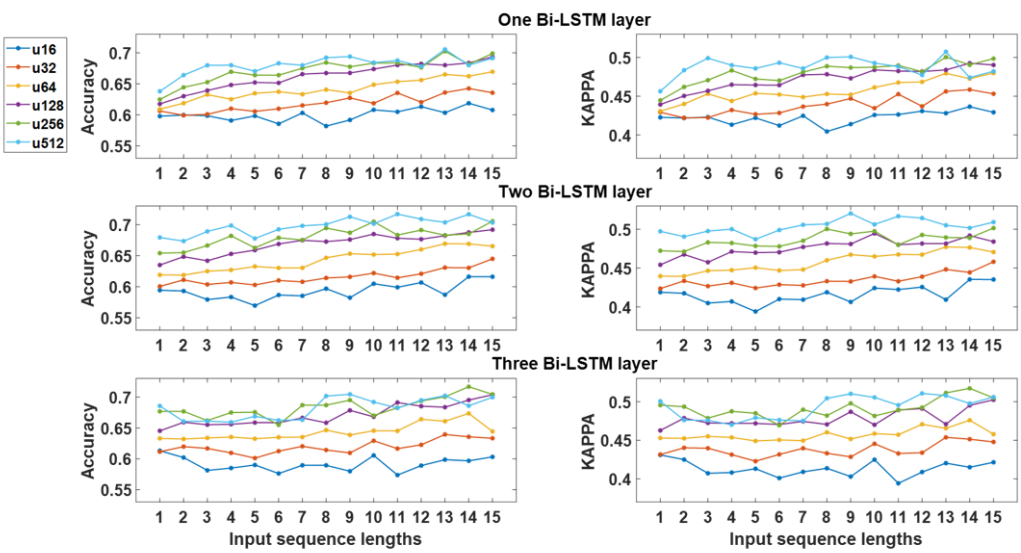


(b)

**Figure 2-3.** Performance of (a) the unidirectional-LSTM model and (b) the bidirectional-LSTM model with the number of layers, input sequence lengths, and units. Accuracy and KAPPA value computed on the validation data. LSTM, long short-term memory; KAPPA, Cohen's kappa coefficient.

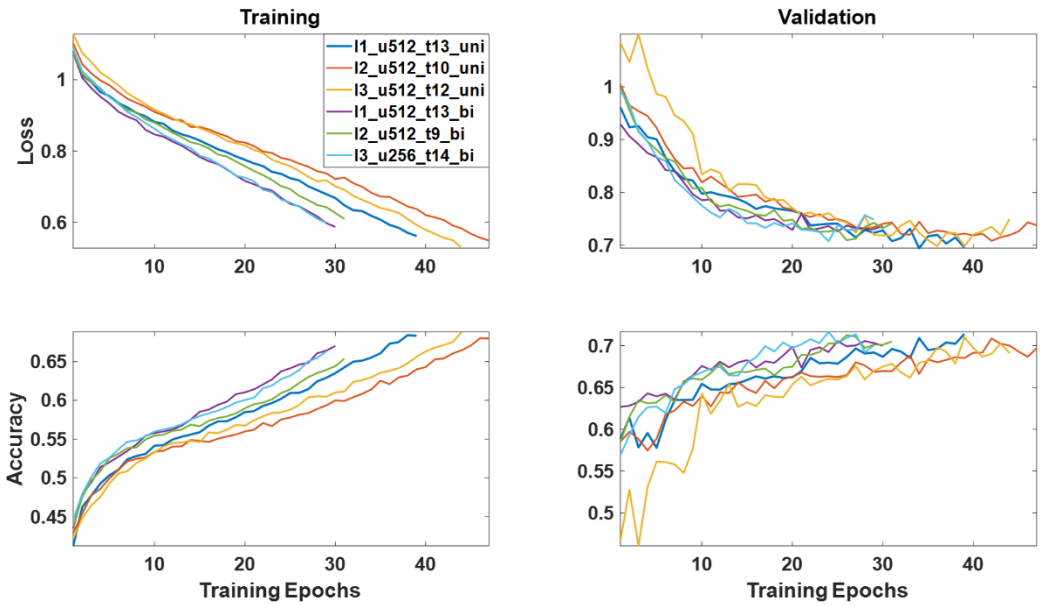


**Figure 2-4.** Learning curves of the LSTM networks. The networks were trained for 50 epochs and an early stopping method was applied. The structure of the model was encoded in the name (see Section 2.1.3). Left, loss and accuracy computed on the training dataset, right: on the validation dataset. LSTM, long short-term memory.

### 2.2.2. Test Dataset Performance

The selected best-performance LSTM model was evaluated on the test dataset—which comprised 20 recordings. The average accuracy and KAPPA values were 0.74 and 0.55, respectively. Table 2-3 summarizes the sleep stage classification performance in each participant and Figure 2-5 shows the scoring results of the sleep stages from the LSTM model and the reference PSG. In the best case, the accuracy and KAPPA were 0.83 and 0.69, respectively. In the worst case, the accuracy and KAPPA were 0.64 and 0.35, respectively. The classification performance of the four sleep stages was computed and compared between the bi-LSTM model and the other machine learning methods, as shown in Figure 2-6. The bi-LSTM model showed the highest performance in sleep stage classification. Furthermore, Figure 2-7 shows each sleep stage classification performance of the proposed model and the machine learning methods. The proposed model showed the highest performance in REM sleep, light sleep, and deep sleep compared to the other methods. In addition, Figure 2-8 presents the confusion matrix of test dataset performance according to each machine learning methods.

**Table 2-3.** Sleep stages classification performance of the selected LSTM model on test dataset

| Participant | Accuracy | KAPPA |
|---|---|---|
| 1 | 0.66 | 0.46 |
| 2 | 0.77 | 0.59 |
| 3 | 0.73 | 0.53 |
| 4 | 0.71 | 0.51 |
| 5 | 0.68 | 0.54 |
| 6 | 0.73 | 0.52 |
| 7 | 0.79 | 0.60 |
| 8 | 0.64 | 0.35 |
| 9 | 0.71 | 0.51 |
| 10 | 0.83 | 0.63 |
| 11 | 0.70 | 0.47 |
| 12 | 0.73 | 0.55 |
| 13 | 0.75 | 0.57 |
| 14 | 0.75 | 0.60 |
| 15 | 0.76 | 0.60 |
| 16 | 0.75 | 0.55 |
| 17 | 0.82 | 0.62 |
| 18 | 0.77 | 0.62 |
| 19 | 0.83 | 0.69 |
| 20 | 0.68 | 0.41 |
| Average | 0.74 | 0.55 |
| S.D. | 0.05 | 0.08 |

LSTM, long short-term memory; KAPPA, Cohen's kappa coefficient; S.D, standard deviation.

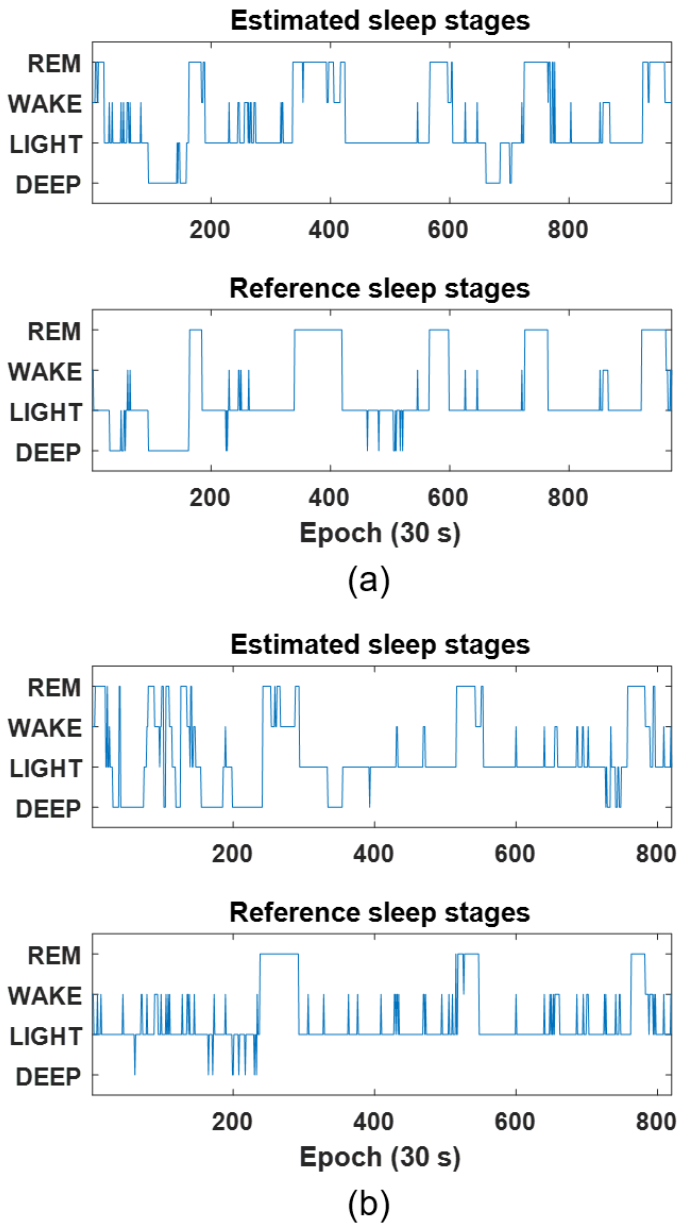


**Figure 2-5.** Epoch-by-epoch sleep stage classification results for (a) best case (participant #19) and (b) worst case (participant #8).

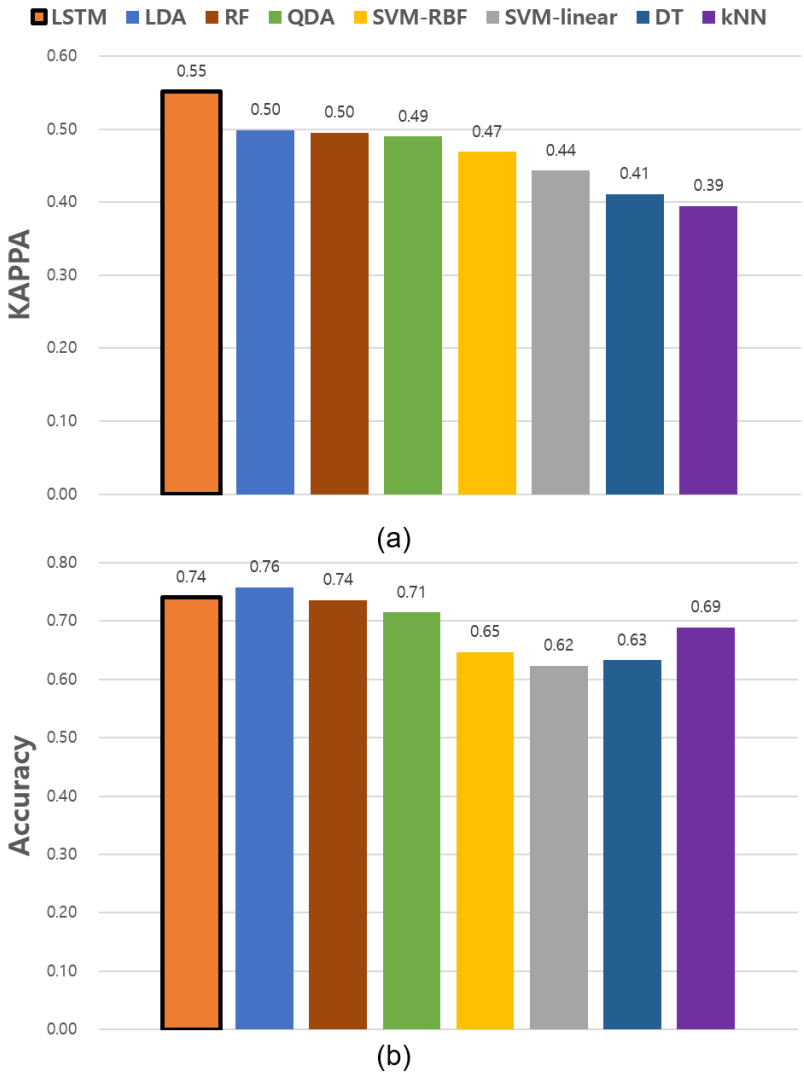


**Figure 2-6.** Performance comparison of the LSTM model with other machine learning methods. kNN, k-nearest neighbors; SVM, support vector machine; LDA, linear discriminant analysis; QDA, quadratic discriminant analysis; DT, decision trees; RF, random forests.

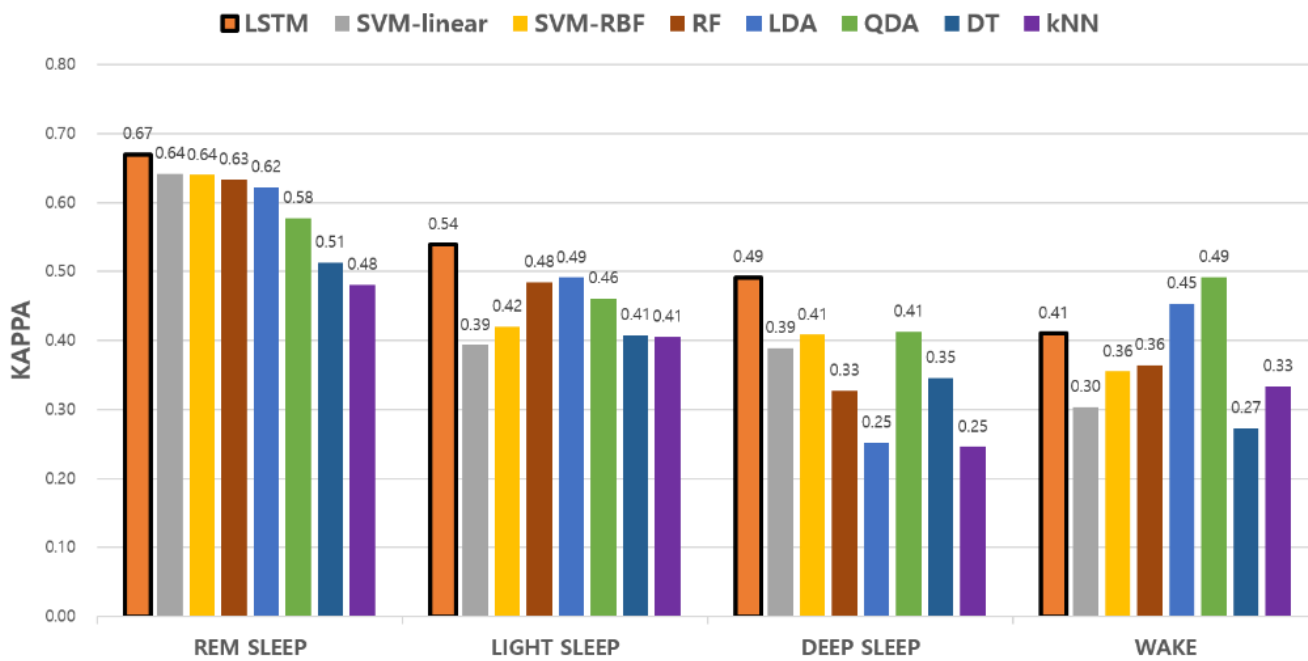


**Figure 2-7.** Comparison of each sleep stage classification performance according to the model. kNN, k-nearest neighbors; SVM, support vector machine; LDA, linear discriminant analysis; QDA, quadratic discriminant analysis; DT, decision trees; RF, random forests.

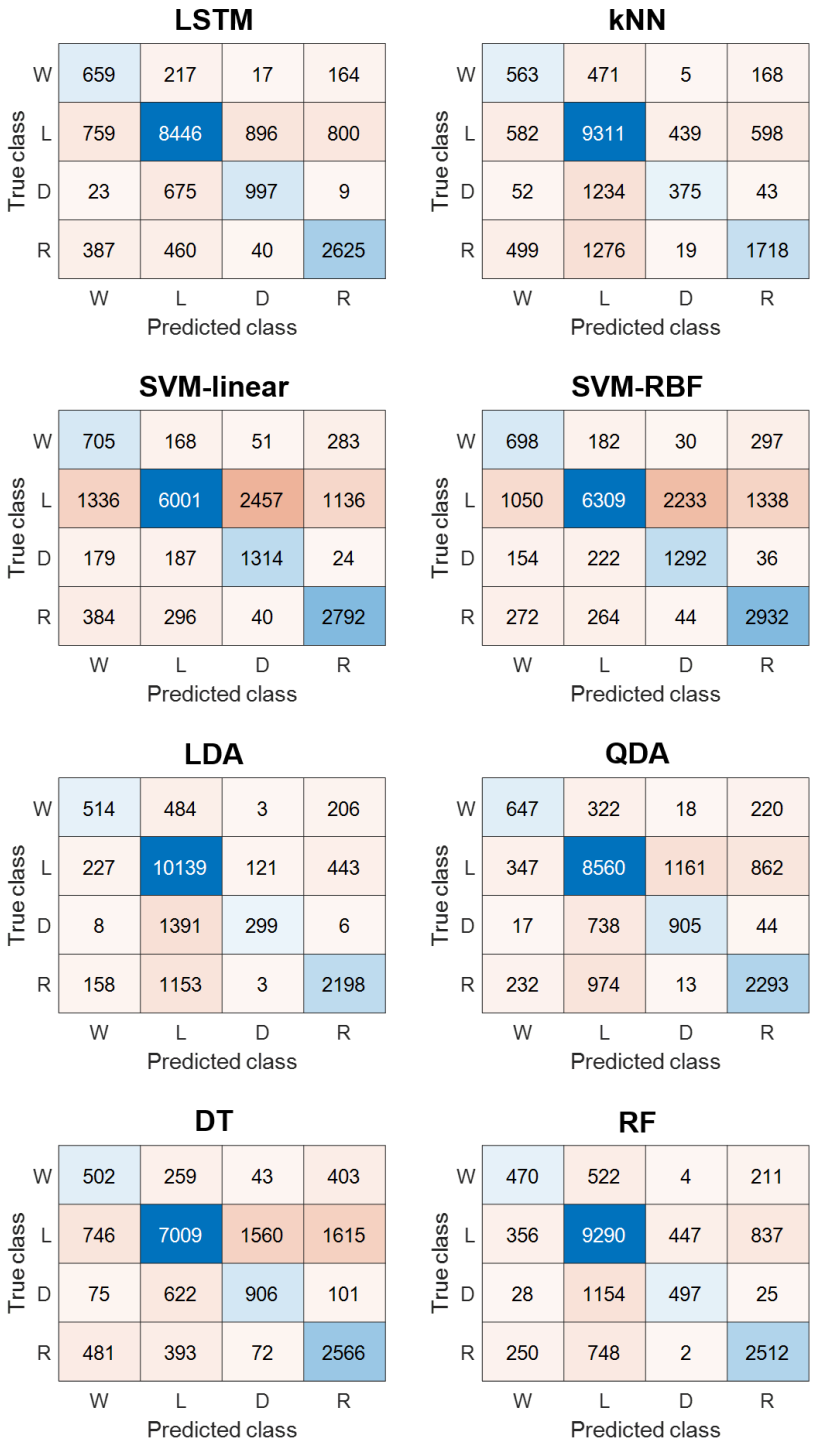


**Figure 2-8.** The Confusion matrix of each machine learning methods. LSTM, long short-term memory; kNN, k-nearest neighbors; SVM, support vector machine; LDA, linear discriminant analysis; QDA, quadratic discriminant analysis; DT, decision trees; RF, random forests.

## 2.3. Discussion

In this study, an optimal LSTM model was proposed to classify four sleep stages using unconstrainedly measured BCG signal. Sixteen sleep-related parameters were extracted from BCG signal and classification performance was evaluated based on the combination of LSTM hyperparameters. Furthermore, the performance of the proposed model was compared with conventional machine learning methods.

### 2.3.1. Performance Evaluation

First, when comparing the performance of the combination of the LSTM hyperparameters, the classification performance tended to increase as the number of input sequence length increased. The input sequence lengths indicate how long lagged observations would be used to predict the current time step. The most representative ability of LSTM networks is that they can store state information and enable long-term dependencies.

Local temporal information is a key factor for sleep stage scoring. Sleep technologists and sleep clinicians consider the sequences of epochs according to the scoring manuals for classifying sleep stages. Modulation of respiration and ANS activity depending on the sleep stages have been well researched [40]–[44], [106], [107]. In addition, the trend of the HRV variations was used as a parameter for sleep stage classification in previous studies [45], [48], [49], [108]–[110]. Therefore, it was assumed that a longer input sequence contains useful information related to the sleep stage, and the LSTM network was considered as an effective model to extract those characteristics.

Indeed, as the input length increased, the performance increased; in addition,

the input sequence length chosen for the final model was nine, which means that the parameters extracted from 270 s BCG signals were used. It is considered that the selected input length reflects long-term information which is a trend of ANS change, and short-term information such as movement or HR. Above a certain input sequence length, useful features for classifying sleep stages may no longer be extracted, or abnormal features may have been extracted.

Further, the classification performance tended to increase as the number of LSTM units increased. The number of units affects the capability of the LSTM cell to capture features of the input sequence. Because 16 parameters were used, the classification performance was compared by doubling the number of units from 16 to 512. As the number of units increased, the performance improved. Increasing the number of units from 128 to 512 showed lower performance improvement than when increasing from 16 to 128. The main reason for the differential performance improvement may be that the main features that differentiate the sleep stages are extracted within 128 units, and the features that can classify the sleep stages more precisely are extracted in the additional units.

Furthermore, the classification performance between unidirectional- and bidirectional-LSTM structures was compared. Bidirectional-LSTM [111] is an extended version of unidirectional-LSTM, which consists of two LSTM model processing forward and backward input sequences independently. This structure can extract information from past and future states simultaneously. The sleep stages are associated with ANS regulation [40]–[43] and affected by the variations of past ANS activity; they affect future ANS activity as well. Therefore, the bidirectional-LSTM model, which extracts past and future state information, could classify sleep stages

better than the unidirectional-LSTM model. Indeed, the bidirectional-LSTM structure showed higher classification performance than unidirectional-LSTM.

When training the LSTM model, different weights were assigned to each class using a previous method [96]. Each sleep stage was not equally distributed in the training dataset, and if the model was trained in the class imbalance state, the model would be learned to classify only for the majority of sleep stages. To prevent the model from overfitting, the class has to be maintained in a balanced state in the training dataset. The performance of the model was compared when using the class-balance state or class-imbalance state. As shown in Figure 2-9, the model trained by the class-balancing method showed a higher classification performance than the model trained by the class-imbalance state. In particular, as shown in the deep sleep classification performance, the former model was trained to differentiate deep sleep, which comprises the smallest portion of 9.0% among the four sleep stages, whereas the latter model could not differentiate deep sleep at all.

Because deep learning is known as a black box, it is difficult to interpret compared to other machine learning methods. However, which parameters are important for the sleep stage classification was examined as following ways. The value of BCG parameters was set to zero, one by one, and then the model was trained and evaluated the performance of sleep stage classification. Figure 2-10 shows the reduction of sleep stage classification performance according to the excluding parameters, which indicate the ranking of parameters useful for classifying sleep stage. Movement and frequency domain HRV parameters were most important to classify sleep stage. These results present indirectly which BCG parameters are important for sleep stage classification.

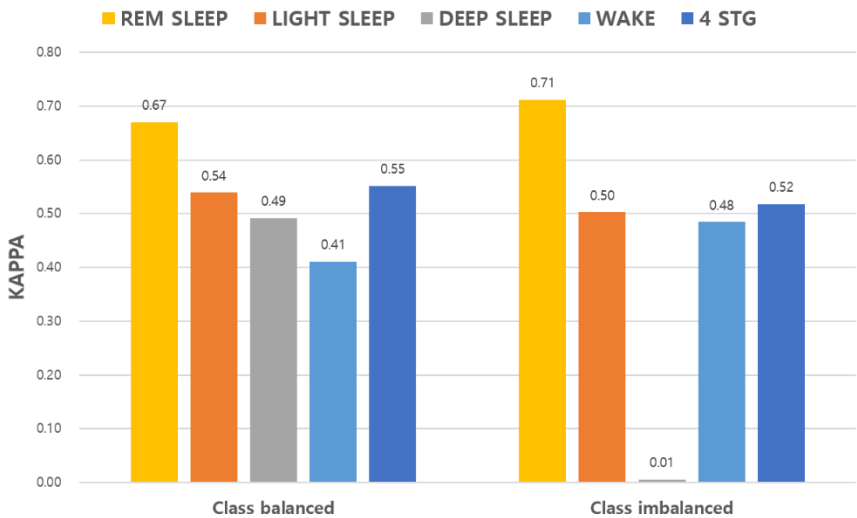


**Figure 2-9.** Comparison of sleep stage classification performance according to the model trained by class-balanced or class-imbalanced dataset. KAPPA, cohen's kappa coefficient.

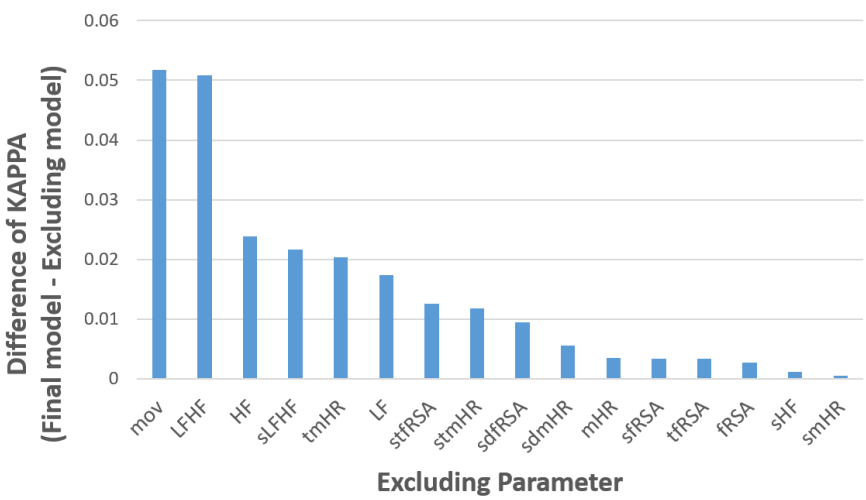


**Figure 2-10.** Reduction of the proposed LSTM model classification performance according to the excluding parameter. KAPPA, cohen's kappa coefficient.

### 2.3.2. Performance Comparison with Other Machine Learning Methods

The proposed LSTM model performance was compared with the conventional machine learning methods such as kNN, SVM, LDA, QDA, DT, and RF. The same parameters that were extracted from the BCG signal were used to train each method model, and the LSTM model was found to be a better method for extracting useful features for sleep staging compared to the other methods.

Figure 2-6 depicts the sleep stage classification performance of the proposed LSTM model and other machine learning methods; the LSTM method produced the highest KAPPA value compared with the other methods. The LSTM model performance was highest for KAPPA values, but not for accuracy. Although the accuracy of the LDA model was higher than that of LSTM model, chance agreement was also higher. Consequently, the KAPPA value of the LDA model was lower than that of the LSTM model. The KAPPA value takes into account the possibility of the agreement occurring by chance and includes each sleep stage classification performance. As shown in Figure 2-7, the LSTM model gave a high performance for each sleep stage classification, whereas the LDA method produced very low performance for deep sleep classification. As a result, the KAPPA value of the LSTM model was the highest.

For each sleep stage, LSTM gave the highest classification performance for light sleep, deep sleep, and REM sleep scoring (see Figure 2-7). In particular, although other machine learning methods were trained by applying the class-balance method, the LSTM model showed the best classification performance for deep sleep, which comprises the smallest proportion of the training dataset. Therefore, the LSTM model could extract more meaningful discrimination features for each sleep

stage than other methods, and it is thus considered the best approach for sleep stage classification.

### 2.3.3. Comparison with Previous Studies

The classification performance of the proposed LSTM model was compared with previous works. Since there are not many studies using BCG signals, the results were compared with studies that used ANS-related parameters from various signals and focused on the classification of four sleep stages. Table 2-4 summarizes and compares the results of this study with previous studies. Isa *et al*. [109] applied kernel dimensionality reduction to classify four sleep stages classification. They extracted HRV features from ECG signals and used the RF method, but the average KAPPA value for four sleep stage estimation was 0.26. Fonseca *et al*. [108] classified four sleep stage using cardiorespiratory features extracted from respiratory inductance plethysmography (RIP) and ECG. Eighty features and the LDA method were used to evaluate the classification performance. Their results showed an accuracy of 0.69 and KAPPA of 0.49. Hender *et al*. [49] assessed an algorithm of sleep stages classification using PAT, pulse oximetry (PO), and ACT signals from a portable monitor Watch-PAT100. While they used multiple signals and acquired a classification KAPPA of 0.48, the proposed LSTM method used only one BCG signal and showed a classification KAPPA of 0.55. The results of previous work [112], which used respiratory dynamic and body movement from BCG signal, are lower than those in the present work, indicating that the LSTM model can lead to improvements in the sleep stage classification performance. These results suggest that the proposed model was appropriate for sleep stages classification.

**Table 2-4.** Performance comparison between previous studies and proposed method for four classes classification

| Study | Sensor type | N | Classifier | Accuracy | Kappa |
|---|---|---|---|---|---|
| Isa *et al* [109] | ECG | 16 | RF | 0.60 | 0.26 |
| Fonseca *et al* [108] | RIP, ECG | 48 | LDA | 0.69 | 0.49 |
| Hender *et al* [49] | PAT, PO, ACT | 227 | Threshold | 0.66 | 0.48 |
| Hwang *et al* [112] | BCG | 20 | Threshold | 0.71 | 0.48 |
| **This stuudy** | **BCG** | **20** | **LSTM** | **0.74** | **0.55** |

ECG, electrocardiogram; RIP, respiratory inductance plethysmography; PAT, peripheral arterial tone; PO, pulse oximetry; ACT, actigraphy; BCG, ballistocardiography; RF, random forest; LDA, linear discriminant analysis; LSTM,

### 2.3.4. Limitations

Even though the results are encouraging, there are some limitations. First, the model was trained and evaluated using BCG signals of only healthy participants. To obtain a generalized model, it is necessary to acquire sleep disorders people data such as insomnia, obstructive sleep apnea, and PLMS and test the model performance. Second, the LSTM model was trained using movement and ANS-related parameters extracted from unconstrained signals, and it might not perform well with other signals such as ECG and PPG. To explore the applicability of other signals, there needs to verify that the parameters used in BCG could be extracted equally from other signals. After then the proposed model could be applied to other modalities by fine-tuning or re-training. Third, although LSTM model improved sleep stage classification performance, model complexity was also increased compared with other machine learning methods. In this study, performance improvement was focused rather than on the complexity of the model. From a computing perspective, there needs to think about the tradeoff between model performance and complexity, and study the way of reducing deep learning model complexity. Finally, the LSTM networks were trained and tested using data recorded in a laboratory environment. In a real-world environment, variables that are not considered in a laboratory environment may occur, and the signal quality could be poor. Thus, methods to obtain BCG signals in real-world environments and evaluate classification performance need to be developed.

# 3

# Comparison of Effects on Heart Rhythm according to External Stimulation Methods during Sleep

An unconstrained sleep monitoring model using LSTM networks was investigated in the previous chapter, in which it was concluded that the LSTM model achieved the best classification performance compared with other machine learning methods and previous works. To enhance sleep quality and promote health levels through sleep, there needs a sleep modulation method that extends beyond passive sleep monitoring. For this purpose, the effects of stimulation methods on heart rhythms are investigated in this chapter, particularly, modulation of ANS is studied. In this thesis, the modulation term is used to mean 'the exertion of a changing or controlling influence on something'. Effects of open-loop vibration stimulation on sleep are assessed according to the sleep macrostructure and HRV analysis. To increase interaction effects between HR and vibration stimulus, the effects of closed-loop stimulation approach on heart rhythm have investigated during naps. In addition, the effect of the vibration stimulation method is compared with other stimulation methods such as auditory and current.

## 3.1. Effect of Open-Loop Vibration Stimulation on Sleep

## 3.1.1. Methods

### 3.1.1.1. Experimental Design and Procedure

Six volunteers (three men, three women; mean age 23.7 years ± 3.0 s.d.; mean BMI 19.9 kg/m$^2$ ± 2.3 s.d.) participated in this experiments. Participants were recruited from posting leaflets on the school bulletin board and this prospective cohort study was approved by the Institutional Review Board of Seoul National University Hospital (IRB No. C-1707-075-869). All participants were healthy and had no sleep-related symptoms. Each participant conducted a consecutive three-day sleep experiment which consisted of one adaptation condition and two experimental conditions. To be accustomed to the sleeping environment, participants conducted an adaptation night at the Center for Sleep and Chronobiology of Seoul National University Hospital. In this condition, only ECG signal was recorded using a wireless device (BN-RSPEC; Biopac Systems, Inc., CA, USA) at the Lead 2 position.

Each participants was tested in two experimental conditions, a stimulation condition (STIM) and a no stimulation condition (SHAM). The order of two conditions was randomized. During the STIM condition, vibration stimulus was applied to the participants during night. The beats per minute (BPM) of the stimulus was set based on the participant's stabilized HR during the adaptation condition. A woofer was used as the vibrator and installed between the mattress and the mattress topper. During two experimental conditions, clinical PSG was conducted. To evaluate the effects of the open-loop vibration stimulus on sleep, sleep macrostructure, HRV, and EEG spectral analysis was conducted in the SHAM and the STIM conditions.

#### 3.1.1.2. Sleep Macrostructure Analysis

The effect of closed-loop stimulation in modulating sleep architecture was examined by computing sleep macrostructure parameters. From PSG recordings, sleep stages were scored by a sleep technologist and verified by a sleep physician according to the AASM manual [21]. Sleep stage scored as wakefulness stage (W), REM, and non-REM sleep stage 1, 2, and 3 (N1, N2, and N3). When they scored and verified sleep stages, the experimental conditions were blinded. From scored sleep stages, fourteen sleep macrostructure parameters were extracted as follows: total recording time (TRT; 'light out' to 'light on' in min), total sleep time (TST; in min), sleep efficiency (SE; (TST/TRT)x100), sleep onset latency (SOL; 'light out' to first epoch of any sleep stage in min), wake after sleep onset (WASO), time and percentage spent in each sleep stage, and sleep fragmentation index (SFI; the total number of awakening and transitions to N1 from N2, N3, or R divided by TST in h). Then the statistical difference of sleep macrostructure parameters was compared between SHAM and STIM condition.

#### 3.1.1.3. Heart Rate Variability Analysis

To evaluate the effect of closed-loop stimulation on the ANS during sleep, HRV and synchronization ratio were analyzed in each sleep stage. The HRV parameters, which is used to investigate the ANS activity, were extracted [113]. To remove noise and baseline drift, the ECG signals were filtered through high-pass filtering (cutoff frequency: 0.5 Hz) and were then sequentially low-pass filtered (cutoff frequency: 30 Hz, 5th order, infinite impulse response, Butterworth). The ECG R-peaks were detected using a self-developed automatic peak detection algorithm [114] and then

manually corrected. Finally, the following conventional HRV parameters were extracted in time and frequency domains. Four time-domain parameters—mean of HR (mHR), percentage of successive R peak-to-R peak (RR) intervals differing by more than 50 ms (pNN50), SD of the RR intervals (SDNN), and root mean square of successive RR-interval differences (RMSSD)—were computed. Furthermore, the HRV parameters were extracted in the frequency domain. First, cubic interpolation was applied to the RR intervals; then, the spectral power was computed using FFT. The spectral power in the frequency ranges of 0.04–0.15 Hz (LF) and 0.15–0.4 Hz (HF) were calculated. Normalized LF and HF were computed by dividing by the sum of the LF and HF. In addition, the ratio of the LF power to the HF power (LF/HF) was extracted. Seven HRV parameters were computed every 5 min in each stage such as WASO, N1, N2, N3, and REM sleep.

#### 3.1.1.4. Statistical Analysis

To verify the effect of the stimulation, a Wilcoxon signed-rank sum test—a nonparametric statistical analysis—was employed because the data were not normally distributed. A p-value of less than 0.05 was considered significant. The statistical analysis was performed using the SPSS statistics program (v. 25.0, SPSS Inc., Chicago, Illinois, USA).

## 3.1.2. Results

### 3.1.2.1. Sleep Macrostructure Results

Figure 3-1 presents the mean values of each sleep structure parameter. In sleep macrostructure analysis, the SOL parameter was significantly decreased in the STIM condition compared to the SHAM condition ($p<0.05$, Wilcoxon rank-sum test).

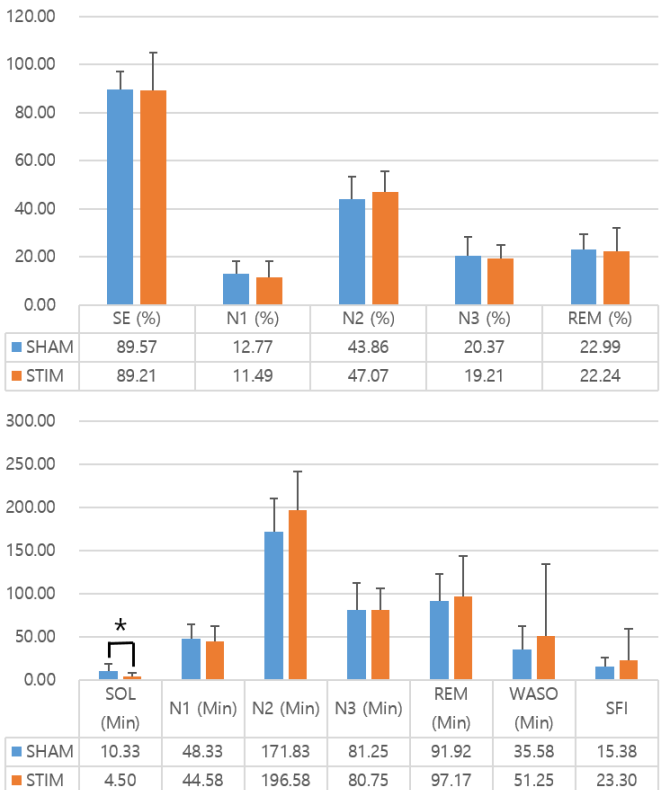


**Figure 3-1.** Effects of open-loop stimulation on sleep macrostructure. Mean (± s.d.) sleep macrostructure parameters during the SHAM and STIM conditions. *$p<0.05$ between the SHAM and STIM conditions (Wilcoxon rank-sum test). SE, sleep efficiency; SOL, sleep onset latency; WASO, wake after sleep onset; SFI, sleep fragmentation index.

#### 3.1.2.2. Heart Rate Variability Results

Table 3-1 summarizes the time- and frequency-domain HRV parameters according to each stage. In the time-domain parameters, the Mean HR under the STIM condition was significantly higher than under the SHAM condition in N3 and REM stage ($p<0.05$, Wilcoxon rank-sum test). There was no significant difference in the frequency-domain HRV parameters for the SHAM and STIM conditions.

**Table 3-1.** Effects of open-loop stimulation on heart rate variability
(Mean ± Standard Deviation)

| Stage & Condition /Variable | | Mean HR | pNN50 | SDNN | RMSSD | nLF | nHF | LF/HF |
|---|---|---|---|---|---|---|---|---|
| WASO | SHAM | 61.38 ±3.05 | 16.09 ±3.52 | 275.4 ±225.4 | 283.8 ±326.2 | 0.66 ±0.11 | 0.34 ±0.11 | 2.84 ±1.65 |
| | STIM | 61.54 ±3.21 | 17.58 ±4.23 | 138.2 ±50.4 | 89.51 ±65.68 | 0.64 ±0.13 | 0.36 ±0.13 | 2.57 ±1.43 |
| N1 | SHAM | 58.56 ±2.59 | 16.76 ±4.88 | 105.2 ±8.7 | 58.47 ±11.04 | 0.63 ±0.08 | 0.37 ±0.08 | 2.18 ±0.82 |
| | STIM | 60.13 ±1.99 | 16.51 ±4.47 | 104.8 ±20.5 | 58.62 ±13.30 | 0.63 ±0.10 | 0.37 ±0.10 | 2.32 ±1.12 |
| N2 | SHAM | 55.12 ±2.98 | 19.25 ±7.49 | 81.09 ±11.67 | 61.94 ±17.36 | 0.49 ±0.09 | 0.51 ±0.09 | 1.32 ±0.48 |
| | STIM | 56.86 ±2.08 | 18.27 ±5.91 | 78.74 ±18.07 | 58.42 ±13.81 | 0.49 ±0.08 | 0.51 ±0.08 | 1.27 ±0.47 |
| N3 | SHAM | **54.82 ±3.27** | 18.99 ±8.62 | 48.67 ±9.80 | 55.34 ±14.78 | 0.30 ±0.08 | 0.70 ±0.08 | 0.48 ±0.18 |
| | STIM | **57.48 ±3.53*** | 17.73 ±6.35 | 49.21 ±6.81 | 53.46 ±10.00 | 0.32 ±0.05 | 0.68 ±0.05 | 0.53 ±0.12 |
| REM | SHAM | **58.24 ±3.81** | 13.89 ±7.01 | 80.29 ±11.90 | 52.35 ±15.98 | 0.62 ±0.08 | 0.38 ±0.08 | 2.01 ±0.62 |
| | STIM | **60.69 ±2.56*** | 12.46 ±5.10 | 80.73 ±11.89 | 50.64 ±12.67 | 0.63 ±0.10 | 0.37 ±0.10 | 2.22 ±1.09 |

HR, heart rate; pNN50, percentage of successive RR intervals that differ by more than 50 ms; SDNN, standard deviation of the RR intervals; RMSSD, root mean square of the successive RR interval differences; nLF, normalized low-frequency band power; nHF, normalized high-frequency band power; LF/HF, ratio of the low-frequency power to the high-frequency power. *$p<0.05$ between the SHAM and STIM conditions (Wilcoxon rank-sum test).

## 3.2. Effect of Closed-Loop Vibration Stimulation on Heart Rhythm during Naps

### 3.2.1. Methods

#### 3.2.1.1. Closed-Loop Vibration System

Figures 3-2 and 3-3 show experimental system and a block diagram of the closed-loop three-stage processes, respectively. Stage 1 includes the measurement of the ECG signal and a band-pass digital filter. The ECG signal was recorded using a wireless device (BN-RSPEC; Biopac Systems, Inc., CA, USA) at the Lead 2 position, and the sampling rate was set to 500 Hz. Then, the ECG signal was filtered between 7 and 25 Hz. In Stage 2, the real-time HR was computed from the ECG signal. In this study, the ECG R-peak detection method based on the Shannon entropy was applied [115]. The filtered ECG signal was normalized, and the Shannon entropy was computed. If the Shannon entropy of a sample was higher than the threshold value, that sample was considered as the R-peak. The HR was calculated from the difference in the R-peak indices; then, the mean HR was computed every 5 min. The mean and SD of absolute errors between the HR extracted from the R-peak using the automatic algorithm [114]—and corrected manually—and the real-time HR were 0.17 and 1.61 bpm, respectively. Furthermore, the real-time R-peak detection accuracy was 99.5%, which is an acceptable level of performance for a real-time peak detection algorithm. In Stage 3, the value of −n% stimulus BPM was computed on the basis of the mean HR calculated over the previous 5 min, and a vibration stimulus was generated. The hypothesis was that an external stimulus with a rate lower than the HR could decrease the heart rhythm rate. Subsequently, an experiment considering stimulation conditions of −3%, −5%, and −10% in frequency was

conducted. A woofer was used as the vibrator and installed between the mattress and the mattress topper, as shown in Figure 3-2(b). The vibrator was positioned such that it was near the participant's heart when the participant was lying on the bed. ECG signals were collected in real time through an NI-DAQ device (USB-6003; National Instruments, TX, USA), and a LABVIEW program (version 15.0.1) was used to compute the HR and stimulus BPM. The aforementioned three steps were repeated in a closed-loop manner, and the stimulus BPM was updated every 5 min.

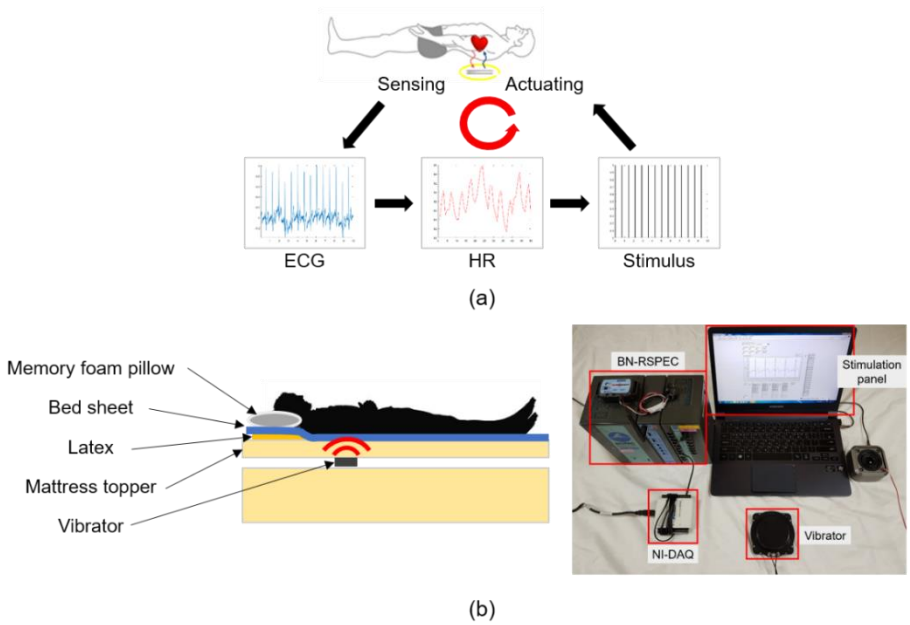


**Figure 3-2.** (a) Developed system consisting of ECG recording, HR detection, and stimulus actuation. These processes are repeated in a closed-loop manner. (b) Closed-loop vibration system diagram and devices used in the experiment. ECG, electrocardiogram; HR, heart rate.

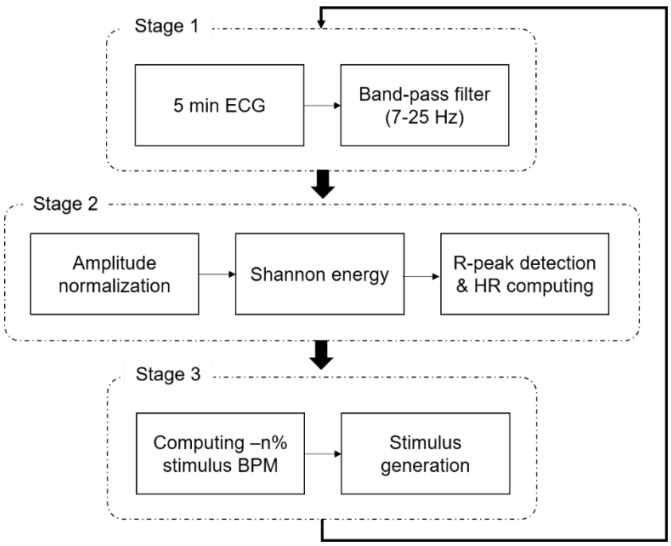


**Figure 3-3.** Block diagram of the closed-loop processes.

### 3.2.1.2. Experimental Design and Procedure

The study was conducted in accordance with the Declaration of Helsinki, and the Institutional Review Board of Seoul National University Hospital approved this prospective cohort study (IRB No. C-1805-165-948). Participants were recruited by posting leaflets on the school bulletin board. Before proceeding with the experiment, a questionnaire was collected to ensure that each participant met the inclusion and exclusion criteria of the experiment. The inclusion criteria for this study were as follows: the participant (1) had to be 18–40 years of age and (2) must be healthy with no symptoms related to sleep. The exclusion criteria for this study were as follows: people (1) with a history of severe physical or psychological illnesses, (2) suffering from arrhythmia, (3) taking medicines that affect sleep, (4) who have consumed alcohol in the three days prior to the experiment, and (5) who suffered from irregular sleep in the three days before the experiment. Ten people (six men, four women) who satisfied the inclusion and exclusion criteria participated in the experiments. All

participants were briefed about the methods and procedure of this study and signed informed consent forms. The mean and SD of the participants' ages were 27.1 and 3.3 years, respectively (Min.–Max.: 22–32 years). The mean and SD of the participants' BMI were 22.2 and 2.4 kg/m$^2$, respectively (Min.–Max.: 17.9–26.7 kg/m$^2$).

Each volunteer participated in one baseline condition and three stimulation conditions, for which the stimulus BPM percentage was set to −3%, −5%, and −10%. To detune the rates between the HR and the weak noninvasive forcing, the ±5% stimulus was considered appropriate in a previous study [84]. The hypothesis was that a negative percentage is appropriate for decreasing the HR and stabilizing the ANS. Thus, stimulus detuning conditions of −3%, −5%, and −10% in frequency were considered. The stimulation experiments were conducted in a random order. Each experiment was conducted in an interval of at least one week. All participants were asked to refrain from consuming alcohol for 3 days before the experiment and from consuming caffeine on the day of the experiment. They participated in the experiments after eating lunch and took a nap that was approximately 90 min long. Before conducting stimulation experiments, the intensity of the stimulus was individually adjusted in order to prevent the vibration interfering with sleep. The participants completed questionnaires related to the subjective sleep quality or vibration stimulus after waking up from the nap.

#### 3.2.1.3. Heart Rate Variability & Synchronization Analysis

In this study, three analysis methods were used to evaluate the effect of the closed-loop vibration system. First, the HRV, which is used to investigate the modulation of the autonomic nerve activity as an efficient, noninvasive, and unobtrusive method was analyzed [113]. Following the section 3.1.1.3. methods, seven HRV parameters were computed every 5 min and analyzed the difference of these parameters under the baseline and stimulation conditions.

Second, the synchronization ratio was computed between heartbeats and stimuli. Phase synchronization analysis, which is a measurement of certain relations between the phases and frequencies of interacting systems, was conducted [116]. In this study, the phase synchronization ratio between heartbeats and stimuli was computed by using the synchrogram method [116]–[118]. It is a visualization tool used to detect the synchronization epochs between two signals. As such, phase-synchronization epochs were detected where the variation in the points was maintained within $\delta = 2\pi/(n\Delta)$ and prolonged for $T$ seconds, as shown in Figure 3-4. In this analyses, the value of $\Delta$ was set to 5, and $T$ was set to 30 s, which is the standard window size for sleep analysis. The synchronization epochs were detected only under the 1:1 ratio condition for heartbeats:stimuli. The surrogate data were constructed from the baseline data to check the effect of vibration stimulation on synchronization. The same rule was applied by which the −n% stimulus BPM is calculated from the previous 5 min mean HR to obtain the stimulus signal for the baseline data. Then, the synchronization ratio was computed from the surrogate data and compared with the synchronization ratio of the stimulation data.

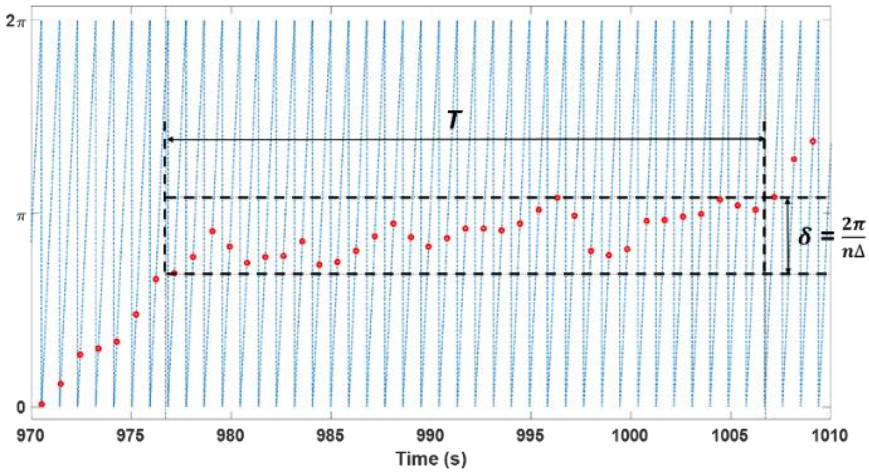


**Figure 3-4.** Phase synchronization and synchrogram method. Each R-peak location of the ECG (red dots) is placed at the corresponding location of the instantaneous phase on the stimulus (blue line). A synchronization epoch is determined for the segment where the variation in the points is maintained within $\delta = 2\pi/(n\Delta)$ and prolonged for $T$ seconds. ECG, electrocardiogram.

### 3.2.1.4. Heart Rate Density Analysis

Finally, the HR density was analyzed to check whether the HR was modulated around the stimulus BPM. A histogram was computed in 0.1 BPM intervals based on the minimum and maximum values of the recorded 5 min HR. Then, the histogram was divided by the total number of heartbeats to extract the HR density. Next, the sum of the densities within ±n BPM was calculated on the basis of the stimulus BPM to confirm the number of heartbeats that was shifted and concentrated on when the stimulus was applied. The green shaded area in Figure 3-5 shows the extracted HR density area. The values of n were set to 0.5, 1.0, and 2.0 BPM.

To compare the results of the baseline and stimulation tests, surrogate stimulus data were required even though there was no stimulus BPM under the baseline condition. The stimulus BPM was computed for the baseline data by using the same rule used to compute −n% stimulus BPM based on the previous 5 min mean HR.

Then, the HR density was compared between the surrogate and stimulus conditions. The HRV, synchronization, and HR density were analyzed using MATLAB R2018b (MathWorks, Natick, MA, USA) software.

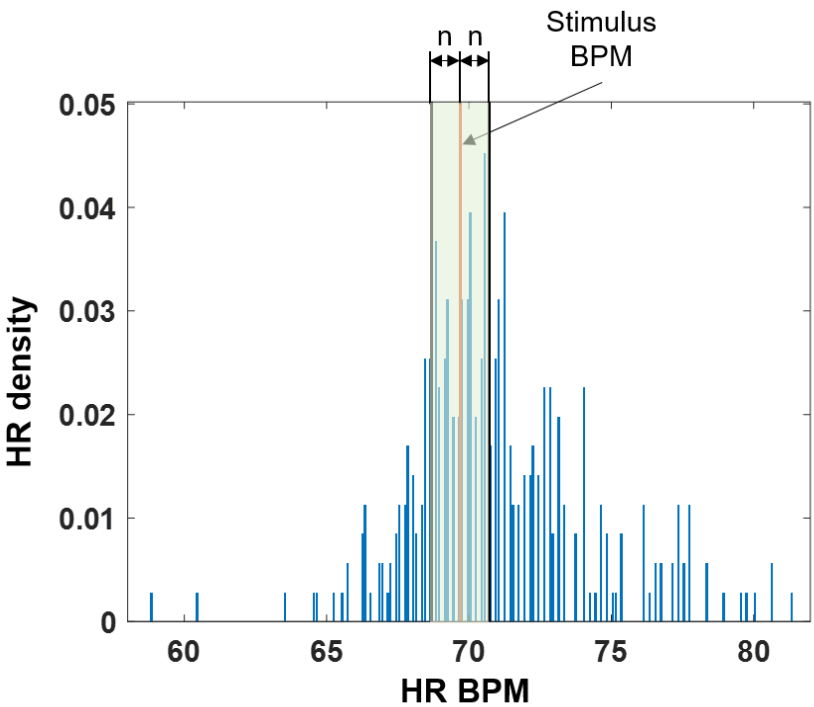


**Figure 3-5.** Example of a heart rate density distribution from Subject 1 under the -3% stimulation condition. The stimulus BPM was computed on the basis of the mean HR calculated over the previous 5 min. Orange line: position of the stimulus BPM. Shaded green: area of the densities between stimulus BPM ± *n* BPM, *n* = 0.5, 1.0, and 2.0 BPM.

### 3.2.1.5. Statistical Analysis

To verify the effect of the stimulation, a Wilcoxon signed-rank sum test—a nonparametric statistical analysis—was employed because the data were not normally distributed. A p-value of less than 0.05 was considered significant. The statistical analysis was performed using the SPSS statistics program (v. 25.0, SPSS Inc., Chicago, Illinois, USA).

## 3.2.2. Results

### 3.2.2.1. Heart Rate Variability Results

Figure 3-6 presents the time- and frequency-domain HRV parameters according to each group. There was no significant difference in the time-domain HRV parameters for the baseline and stimulation conditions. However, in the frequency domain, the nLF and LF/HF ratio parameters were significantly lower under the −3% stimulation condition than under the baseline condition ($p < 0.03$ and 0.01, Wilcoxon signed-rank sum test). In addition, the nHF parameter under the –3% stimulation condition was significantly higher than that under the baseline condition ($p < 0.03$, Wilcoxon signed-rank sum test). Moreover, no significant differences were observed between the HRV parameters for the baseline and −5% or −10% conditions. Table 3-2 presents the average and SD of the HRV parameters according to each condition.

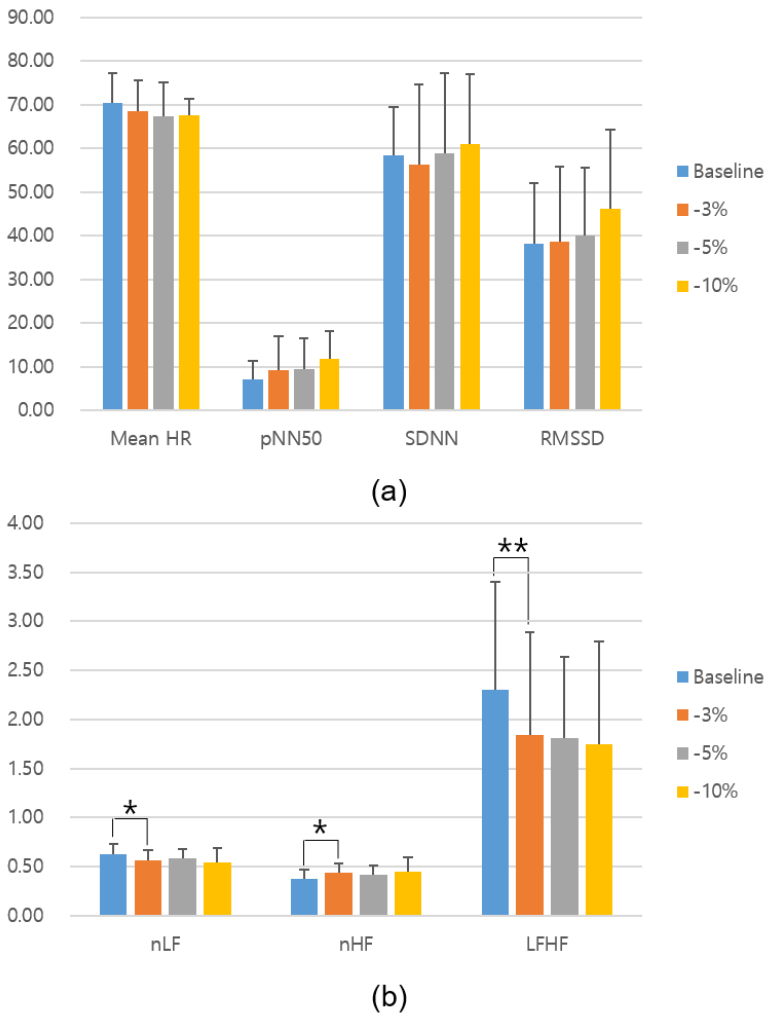


**Figure 3-6.** HRV parameters under each experimental condition: (a) time- and (b) frequency-domain HRV results. *$p < 0.03$ and **$p < 0.01$ between the baseline and stimulation conditions (Wilcoxon rank-sum test). HRV, heart rate variability.

**Table 3-2.** Results of heart rate variability analysis (Mean ± Standard Deviation)

| Group/ Variable | Mean HR | pNN50 | SDNN | RMSSD | nLF | nHF | LF/HF |
|---|---|---|---|---|---|---|---|
| Baseline | 70.38 ± 6.84 | 7.11 ± 4.20 | 58.41 ± 11.03 | 38.15 ± 13.97 | 0.63 ± 0.10 | 0.37 ± 0.10 | 2.30 ± 1.10 |
| −3% | 68.44 ± 7.25 | 9.22 ± 7.64 | 56.19 ± 18.36 | 38.65 ± 17.20 | **0.56 ± 0.10**[a] | **0.44 ± 0.10**[a] | **1.84 ± 1.04**[b] |
| −5% | 67.42 ± 7.67 | 9.52 ± 7.03 | 58.90 ± 18.41 | 39.95 ± 15.64 | 0.58 ± 0.10 | 0.42 ± 0.10 | 1.81 ± 0.83 |
| −10% | 67.54 ± 3.91 | 11.89 ± 6.25 | 61.01 ± 15.89 | 46.26 ± 18.12 | 0.55 ± 0.15 | 0.45 ± 0.15 | 1.75 ± 1.04 |

HR, heart rate; pNN50, percentage of successive NN intervals that differ by more than 50 ms; SDNN, standard deviation of the NN intervals; RMSSD, root mean square of the successive NN interval differences; nLF, normalized low-frequency band power; nHF, normalized high-frequency band power; LF/HF, ratio of the low-frequency power to the high-frequency power.

a: $p < 0.03$ between the baseline and −3% stimulation conditions, b: $p < 0.01$ between the baseline and −3% stimulation conditions (Wilcoxon rank-sum test).

#### 3.2.2.2. Synchronization Analysis Results

The synchronization ratio between heartbeats and stimuli was computed. Table 3-3 presents each participant's synchronization ratio under the stimulation conditions. In general, the results exhibited an increased synchronization in average and in number of participants (7 participants vs 3 participants in -3% stimulation); however, the statistical significance level was not sufficiently low to confirm the synchronization difference between the surrogate and stimulation conditions.

**Table 3-3**. Summary of synchronization ratio under each set of stimulation conditions

| | –3% | | –5% | | –10% | |
|---|---|---|---|---|---|---|
| Subject | Surrogate | Stim | Surrogate | Stim | Surrogate | Stim |
| 1 | 3.28 | 5.03 | 1.37 | 0.69 | 1.21 | 0.74 |
| 2 | 5.15 | 19.12 | 3.65 | 7.76 | 0.00 | 1.00 |
| 3 | 0.59 | 2.97 | 3.38 | 9.34 | 1.55 | 1.12 |
| 4 | 0.57 | 10.11 | 0.00 | 2.52 | 0.00 | 0.00 |
| 5 | 0.65 | 0.00 | 0.63 | 0.00 | 0.00 | 0.00 |
| 6 | 1.12 | 1.26 | 0.00 | 0.59 | 0.00 | 0.00 |
| 7 | 2.95 | 3.73 | 1.21 | 0.00 | 0.00 | 1.05 |
| 8 | 5.23 | 8.91 | 1.13 | 1.17 | 0.00 | 0.00 |
| 9 | 3.84 | 0.56 | 3.32 | 1.36 | 0.00 | 0.00 |
| 10 | 2.62 | 0.75 | 4.63 | 2.48 | 0.57 | 0.67 |
| Average | 2.60 | 5.25 | 1.93 | 2.59 | 0.33 | 0.46 |
| SD | 1.72 | 5.68 | 1.58 | 3.11 | 0.56 | 0.48 |

### 3.2.2.3. Heart Rate Density Results

Figure 3-7 shows the sum of the densities within 0.5 BPM based on the stimulus BPM. In addition, Table 3-4 summarizes the average of the HR densities in each interval. A significant increase was observed between the surrogate and −3% stimulus HR densities. In every interval, the HR BPM densities were significantly higher under the −3% stimulation condition than under the surrogate condition ($p < 0.03$, Wilcoxon signed-rank sum test). However, there was no significant difference between the surrogate and −5% or −10% conditions.

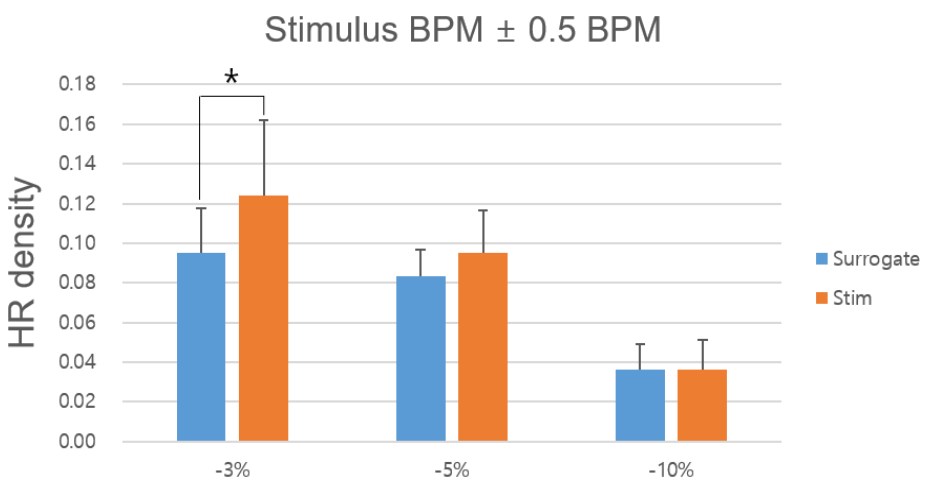


**Figure 3-7.** HR densities in stimulus BPM ± 0.5 BPM for each experimental condition. *$p < 0.01$ between the baseline and stimulation conditions (Wilcoxon rank-sum test). HR, heart rate.

**Table3-4.** Distribution of heart rate densities (Mean ± Standard Deviation)

| Group /Variable | | ±0.5 BPM | ±1 BPM | ±2 BPM |
|---|---|---|---|---|
| –3% | Surrogate | 0.10 ± 0.02 | 0.18 ± 0.04 | 0.35 ± 0.08 |
| | Stim | **0.12 ± 0.04** [a] | **0.23 ± 0.07** [b] | **0.42 ± 0.12** [b] |
| –5% | Surrogate | 0.08 ± 0.01 | 0.16 ± 0.03 | 0.31 ± 0.05 |
| | Stim | 0.10 ± 0.02 | 0.17 ± 0.03 | 0.33 ± 0.05 |
| –10% | Surrogate | 0.04 ± 0.01 | 0.07 ± 0.02 | 0.14 ± 0.05 |
| | Stim | 0.04 ± 0.01 | 0.07 ± 0.03 | 0.14 ± 0.04 |

a: $p < 0.01$ between the surrogate and -3% stimulation conditions, b: $p < 0.03$ between the surrogate and -3% stimulation conditions (Wilcoxon rank-sum test).

## 3.3. Change of Autonomic Nervous System Characteristics according to External Stimulation Methods during Naps

### 3.3.1. Experimental Design and Procedure

In this study, the effects of external stimulation methods, including the closed-loop stimulation method in section 3.2 and previous study methods were compared. Institutional Review Board of Seoul National University Hospital approved this prospective cohort study (IRB No. C-1805-165-948). Seven people (five men, two women) who satisfied the inclusion and exclusion criteria of section 3.2.1.2 participated in the experiments. All participants were briefed about the methods and procedure of this study and signed informed consent forms. The mean and SD of the participants' ages were 25.7 and 2.9 years, respectively (Min.–Max.: 21–30 years). The mean and SD of the participants' BMI were 22.7 and 2.5 kg/m$^2$, respectively (Min.–Max.: 17.9–26.7 kg/m$^2$). All participants were asked to refrain from consuming alcohol for 3 days before the experiment and from consuming caffeine

on the day of the experiment. They participated in the experiments after eating lunch and took a nap about 90 min.

Each participant conducted one baseline condition and three stimulation methods consisting of auditory, current, and closed-loop vibration stimulation. First, auditory stimulation was used based on the previous study [119]. As shown in Figure 3-8, white noise based auditory stimulation consists of a 10-second period signal that combines a 2-s oscillating white noise (15 Hz) with an 8-s constant white noise period. Auditory volume was set to 42 dB corresponding to the library noise and auditory stimulation was induced during the whole napping time using a speaker.

The second stimulation method was electrical stimulation. In previous studies [22], [63], [120], it was shown that rocking bed which stimulating the vestibular system affected sleep. Furthermore, Krystal, Andrew D. *et al* [121] researched the effects of vestibular stimulation for transient insomnia. Although vestibular stimulation did not have a therapeutic effect in a model of transient insomnia, it may shorten SOL. Following this study method, in this study, electrodes were attached over the mastoid position and bilateral currents were induced using stimulator (STM100C; Biopac Systems, Inc., CA, USA). A current of 0.1-0.3 mA was applied at a frequency of 0.5 Hz for 20 minutes after lying on the bed.

The third stimulation method was closed-loop vibration stimulation developed in the previous section 3.2 study. As a result of the previous study, the value of –n% stimulus BPM was set to -3% and vibration stimulation was induced during the whole napping time. The experimental sequence of the three aforementioned stimulation methods was randomized. Each experiment was conducted in an interval of at least one week.

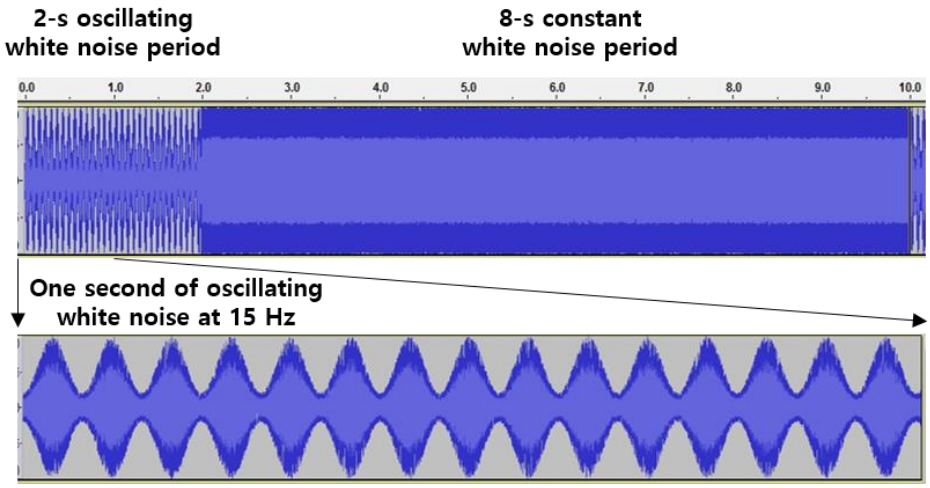


**Figure 3-8.** The example of auditory stimulation signals, which comprising 2-s of white noise oscillating period at 15 Hz followed by 8-s of constant white noise period.

### 3.3.2. Heart Rate Variability Analysis and Results

To compare ANS changes depends on the stimulation methods, HRV analysis was conducted. Following the section 3.1.1.3 methods, seven HRV parameters were extracted in time- and frequency-domain every 5 min and analyzed the difference of these parameters under the baseline and stimulation conditions.

Figure 3-9 presents the time- and frequency-domain HRV parameters according to each condition. There was no significant difference in the time-domain HRV parameters for the baseline and stimulation conditions. However, in the frequency domain, the nLF and LF/HF ratio parameters were significantly lower under the vibration stimulation condition than under the baseline condition ($p < 0.05$ and 0.02, Wilcoxon signed-rank sum test). In addition, the nHF parameter under the vibration stimulation condition was significantly higher than that under the baseline condition ($p < 0.05$, Wilcoxon signed-rank sum test).

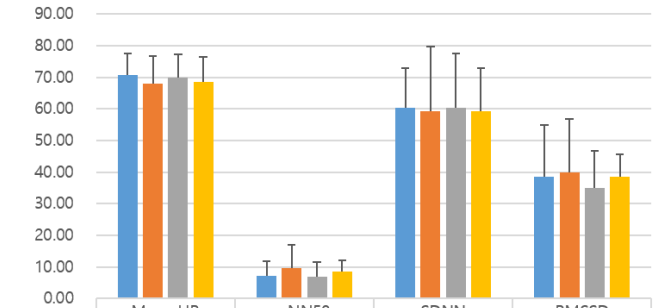


| | Mean HR | pNN50 | SDNN | RMSSD |
|---|---|---|---|---|
| Baseline | 70.68 | 7.11 | 60.29 | 38.50 |
| Vibration | 67.85 | 9.71 | 59.39 | 39.95 |
| Auditory | 69.88 | 6.91 | 60.21 | 35.09 |
| Current | 68.43 | 8.62 | 59.14 | 38.44 |

(a)

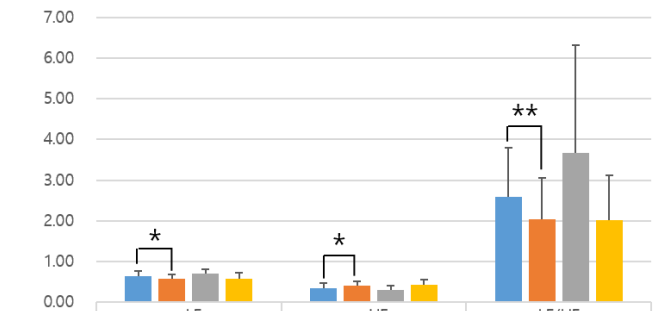


| | nLF | nHF | LF/HF |
|---|---|---|---|
| Baseline | 0.65 | 0.35 | 2.59 |
| Vibration | 0.59 | 0.41 | 2.03 |
| Auditory | 0.70 | 0.30 | 3.67 |
| Current | 0.58 | 0.42 | 2.02 |

(b)

**Figure 3-9.** HRV parameters under each stimulation condition: (a) time- and (b) frequency-domain HRV results. *$p < 0.05$ and **$p < 0.02$ between the baseline and stimulation conditions (Wilcoxon rank-sum test). HRV, heart rate variability.

## 3.4. Discussion

In this study, a new stimulation system was developed and the effects of stimulation methods on the ANS during sleep were compared. First, an open-loop experiment was conducted that was applied with vibration stimulation based on the stable HR measured on the first day. Although SOL parameter was significantly decreased, only six volunteers participated in this study, and HRV analysis showed

no significant difference in the nLF and nHF parameters which indicating the ANS activity. The open-loop vibration stimulation system was developed based on the characteristics of the cardiac system interacting with the external system of periodicity, but did not affect the modulation of the heart rhythm. This result was probably due to the large phase difference gap between the external vibration stimulus and the heart rhythm. In the STIM condition, the mean and SD of gap percentage that computed by the absolute value of the difference percentage between the HR and the stimulus BPM were 11.93 % and 3.27 %, respectively. It is known that if the detuning which is a difference between the two oscillator frequencies is small, then even a very small force can entrain the oscillator [71]. Because of the large detuning between HR and stimulation BPM in this study, it would have been difficult to see the result of heart rhythm modulation by the interaction of the two systems.

Second, to reduce the detuning between two systems and increase the effects on heart rhythm modulation, a novel closed-loop vibration stimulation system was developed. The effect of the developed system on heart rhythm was evaluated during napping. The HRV analysis confirmed a significant difference between the baseline and −3% stimulation conditions. The nHF parameter, which represents the parasympathetic activity [35], significantly increased, and the LF/HF parameter, which represents the sympathovagal balance [113], significantly decreased under the −3% stimulus condition. These results indicate that −3% stimulation makes the ANS more stable. It is possible that the effects of ANS stabilization, such as increased SWS or less sleep-stage transition, may have resulted in more stable sleep. When the HRV was analyzed every 15 min, the nHF parameter for the −3% stimulation

condition significantly increased in the second and third periods (Figure 3-10(a)), and the LF/HF parameter significantly decreased in the third period (Figure 3-10(b)). The second or third period of the HRV corresponds to the SWS time, which normally occurs 20–40 min in the first cycle [122]. Thus, it is possible that the SWS was increased or that the sleep stage was stabilized under the −3% stimulation condition. Compared with the −3% stimulation condition, no significant differences were observed between the corresponding HRV parameters under the baseline and −5% or −10% conditions. Even though the mean HRs of the participants differed under the different experimental conditions listed in Table 3-2, their difference is not statistically significant. Further, frequency-domain HRV parameters, one of main results, under baseline and stimulation conditions were compared after normalization. While the HRs of the participants were different, mean HR was detected every 5 min and applied n% lower BPM stimulus based on previous 5-min mean HRs. The closed-loop stimulation was adopted for this study to reflect the temporal HR variation in real time and minimize the effect of daily mean HR difference. The most appropriate way to conduct stimulations was based on previous mean HRs, as the significance of the stimulation effect does not deteriorate even if the participants have different mean HRs on different days.

In the HR BPM density analysis, the density significantly increased in all intervals under the −3% stimulation condition compared with the surrogate data, which were extracted from the baseline data. This implies that the closed-loop vibration system affects the shifting of heart rhythm around the external stimulus BPM. Furthermore, no significant differences were observed between the surrogate data and the −5% or −10% conditions. Therefore, the −3% stimulation condition is

appropriate for modulating the heart rhythm, and it could be said that an external stimulus closer to the HR has a larger effect on the HR modulation. According to a previous study [84], the ±5% stimulation range is appropriate for detuning between the HR and weak noninvasive forcing. In this study, only the negative percentage conditions were tested to stabilize the heart rhythm. When an external weak stimulation is applied to the heart, which is a self-sustained oscillator, a smaller phase difference is more suitable for modulation. In this study experiment, −3% stimulation was more appropriate than the other values for modulating the heart rhythm.

The synchronization analysis showed no significant differences between the surrogate and stimulation data. Although no statistical difference was observed for the participant-specific synchronization rate, it was found that the synchronization ratios of seven participants increased under the −3% stimulation condition (Table 3-3). However, the synchronization ratio of five and two participants was observed to increase under the −5% and −10% simulation conditions, respectively, compared to the surrogate data. It was expected that if the developed system affected heart rhythm, the HR density and synchronization would be changed. Although the HR densities were significantly increased, the synchronization ratios did not increase in a statistically significant manner. This is because the synchronization analyzes the phase-lock period, which lasted more than $T$ seconds. Although increasing the HR density does not always lead to an increase in the synchronization ratio, there is a significant positive correlation between the HR density and the synchronization ratio (Pearson's correlation coefficient = 0.762, $p < 0.01$). Because the results exhibited the tendency of synchronization, further studies are required with a targeted experimental setup and increased number of participants.

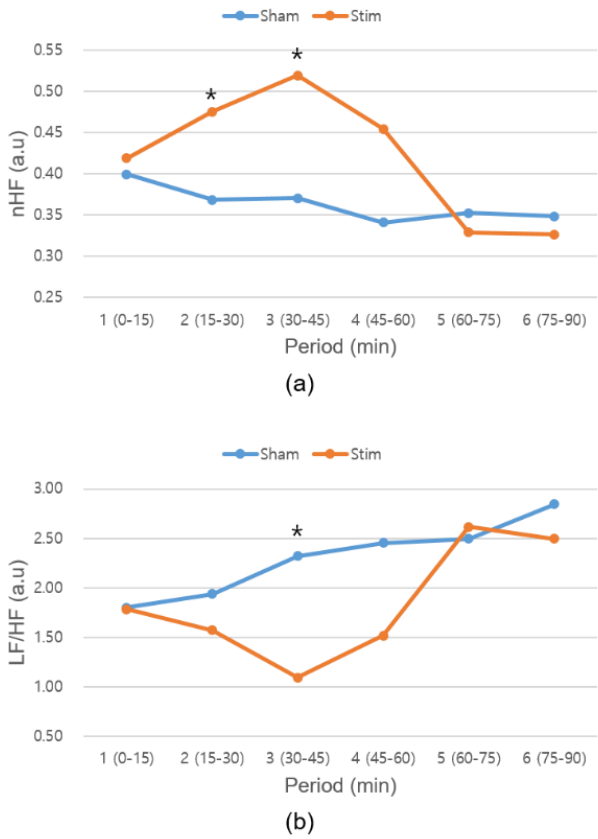


**Figure 3-10.** Results of the HRV extracted every 15 min under the baseline and −3% stimulation conditions: (a) nHF and (b) LF/HF parameter results. HRV, heart rate variability; nHF, normalized high-frequency band power; LF/HF, ratio of the low-frequency power to the high-frequency power.

Finally, when comparing the effects of sleep stimulation methods such as auditory, current, and vibration, the proposed closed-loop stimulation system was more effective to modulate heart rhythm than the other methods. The HRV analysis confirmed a significant difference between the baseline and vibration stimulation conditions. The nHF parameter was significantly increased, and the nLF and LF/HF parameters were significantly decreased under the vibration condition. These results indicate that vibration stimulation method was more effective to stabilize the ANS than the other methods.

**Table 3-5.** Questions about sleep and comfort of the stimulation (Mean ± Standard Deviation)

| Question/Group | Baseline | −3% | −5% | −10% |
|---|---|---|---|---|
| Subjective SOL (Min) | 15.6 ± 8.3 | 14.4 ± 10.9 | 17.2 ± 8.2 | 12.8 ± 6.3 |
| How was the sleep quality?<br>(0–5, No sleep at all–Very good sleep) | 3.4 ± 0.8 | 3.9 ± 1.1 | 4.1 ± 0.8 | 4.1 ± 1.2 |
| Felt external stimuli while sleeping<br>(0–5, felt nothing–felt very well) | 0.1 ± 0.3 | 1.0 ± 1.1 | 0.6 ± 0.8 | 0.7 ± 0.8 |
| I couldn't sleep because of the external stimulus<br>(0–5, No–Yes) | 0.0 ± 0.0 | 0.4 ± 0.9 | 0.5 ± 0.7 | 0.3 ± 0.5 |

SOL, Sleep onset latency, which indicates the time from "lights out" to the first epoch of any sleep stage.

In summary, the closed-loop vibration-stimulation system was most effective when compared to the other methods and affected the modulation of the HR density and the stabilization of the ANS. Specifically, −3% stimulation was more appropriate for modulating heart rhythm than the −5% and −10% cases. Human physiological systems interact with internal subsystems or external systems. Specifically, the rhythm of the cardiac system could be entrained by external weak forcing [84]. Human heart rhythms synchronize, while co-sleeping and the heart rhythm of one co-sleeper can act as an external stimulus that affects the heart rhythm of the other co-sleeper [85]. The results of this study may be attributed to the independent and weak but continuous vibration rhythm system interacting with the cardiac system. Existing stimulation methods for sleep enhancement [9], [10], [65]–[67], [69], [70], [123] could be inconvenient for long-term use, while the proposed system has the advantage of unobtrusive stimulation. As shown in Table 3-5, for the questions related to the discomfort of the stimulation system, no significant differences are observed between the baseline and stimulation conditions. If the HR is detected through the BCG signal by using a sheet-type sensor such as an EmFit or PVDF sensor, which can be unobtrusively installed under the bed sheet, the proposed system could reduce the hassle of attaching the sensor and can comprise a closed stimulating loop in an unobtrusive or unconstrained manner. Therefore, closed-loop stimulation system could be a new method for applying external stimulation during sleep.

The aims of this study were to propose a new system and investigate the effect of stimulation on heart rhythm. However, there are some limitations. First, the proposed system were evaluated with 10 participants and checked the possibility of

modulating their heart rhythms during napping. More participants are needed to evaluate the system during a whole night's sleep pattern. However, although experiments were conducted on only 10 people, the results confirmed the feasibility of applying the proposed system to night sleep. Second, the stimulation effect was examined on heart signals. HR oscillations interact with other mechanisms such as baroreflex or chemoreflex. Grimaldi *et al*. [83] assessed the effect of acoustic stimulation during sleep in HRV, blood pressure (BP), and cortisol. An enhancement in SWA was associated with a reduction in evening-to-morning variation in cortisol levels and indices of sympathetic activity. However, they did not identify an association between BP changes and SWA enhancement as observed in HRV and cortisol. Further investigations are required to clarify the physiological effect of stimulation by measuring BP, cortisol, and $CO_2$ signals.

Third, only healthy people were included in this study. The proposed system could be applicable to persons with arrhythmia who have to utilize a pacemaker—a device that generates electrical stimulation and regulates heart rhythm. The proposed system does not change stimulus BPM by detecting heartbeats in real-time and making contact with the heart directly like a pacemaker, but the methods are similar in that they try to modulate heart rhythm by applying a stimulus. There needs to evaluate the effectiveness of the proposed system on persons with arrhythmia in a future study.

Fourth, the proposed system was tested for approximately 90 min during napping. Generally, one sleep cycle, i.e., NREM–REM sleep, is completed within 90 min. In night sleep, the sleep cycle is repeated approximately 4–5 times, and there needs to evaluate the effect of the proposed system over several sleep cycles. Finally,

the proposed system performance was not compared with those of other stimulation methods. The closed-loop vibration system was developed firstly and utilized it during naps. Not only are there no studies that apply vibration stimulation during naps, there are only studies that apply other stimulation methods conducted using PSG during sleep. To solve these aforementioned issues, the proposed system needs to be evaluated during night sleep by using a PSG test. From the PSG test, it will be able to confirm the changes in sleep stages, which are scored by sleep technologists, and analyze the changes in brain waves or ANS characteristics in each sleep stage.

# 4

# Effects of Closed-Loop Vibration Stimulation on Sleep and Memory

The effects of stimulation methods on heart rhythm during sleep was investigated in the previous chapter. The closed-loop vibration stimulation modulated heart rhythm and stabilized ANS. In addition, it was most effective in modulating the heart rhythm compared with other stimulation methods. In this chapter, closed-loop stimulation method is applied during night sleep. Its stimulation effects on sleep and memory are investigated. Sleep macrostructure, HRV, synchronization, and EEG spectral analysis are conducted to evaluate stimulation effects. Furthermore, the change of memory retention will be investigated and discussed.

## 4.1. Methods

### 4.1.1. Participants and Experimental Procedure

Twelve volunteers (Six men, six women; mean age 29.2 years ± 3.7 s.d.; mean BMI 22.0 kg/m2 ± 2.5 s.d.) participated in the experiments. Participants were recruited from posting leaflets on the school bulletin board and this prospective cohort study was approved by the Institutional Review Board of Seoul National University Hospital (IRB No. C-1809-146-978). The study included only participants who were healthy, had no sleep-related symptoms and aged 18 to under 40. Participants suffering from arrhythmia, taking medicines that affect sleep, who had a history of severe physical or psychological illnesses, and who suffered from irregular sleep in the three days before the experiment were not included in the study. Twelve participants were satisfied with the inclusion criteria and signed informed consent forms of this study. This study procedure is illustrated in Figure 4-1. Prior to the two experimental nights, participants were accustomed to the experimental setup during one adaptation night. Standard clinical PSG recording EEG, EOG, EMG, ECG, and breathing measures [21] was conducted at the Center for Sleep and Chronobiology, Seoul National University Hospital.

Each participant was tested in two experimental conditions, a stimulation condition (STIM) and a no stimulation condition (SHAM). The order of two conditions (STIM or SHAM) was randomized with counterbalanced order across participants. The two experimental conditions were separated by at least one week and not more than 3 weeks. All participants were asked to maintain a regular sleep-wake schedule and refrain from drinking alcohol during the three days before each experimental night. Further, caffeine-containing drinks were not allowed on an

experimental day. On experimental days, participants arrived at 8:00 p.m. and sensors were attached for PSG recordings. Then participants performed on a declarative memory task between 9:30 and 10:30 p.m. After the learning phase, participants were not allowed to use electronic devices until they went to bed to reduce devices' effects on sleep. Next morning, after detaching PSG sensors, participants were examined the recall of memory.

During the STIM condition, vibration stimulus was applied to the participants during night using a previously developed closed-loop stimulation system [124]. The closed-loop stimulation process consists of three steps. First, the ECG signal was recorded from a wireless device (BN-RSPEC; Biopac Systems, Inc., CA, USA) at a sampling frequency of 500 Hz. Second, the real-time HR was computed based on the Shannon entropy method for detecting ECG R-peak. Finally, a vibration stimulus was generated after the value of −3% stimulus BPM was calculated on the basis of the mean HR computed over the previous 5 min. These processes repeated as a closed-loop manner and stimulus BPM was updated every 5 mins. In the SHAM condition, the same procedures were applied except that stimulation volume was muted. The intensity of the stimulus was individually adjusted before conducting PSG recordings and the comfort of sleep and stimulation were evaluated by a five-point scale in the morning.

#### 4.1.2. Sleep Macrostructure Analysis

The content is the same with Section 3.1.1.2.

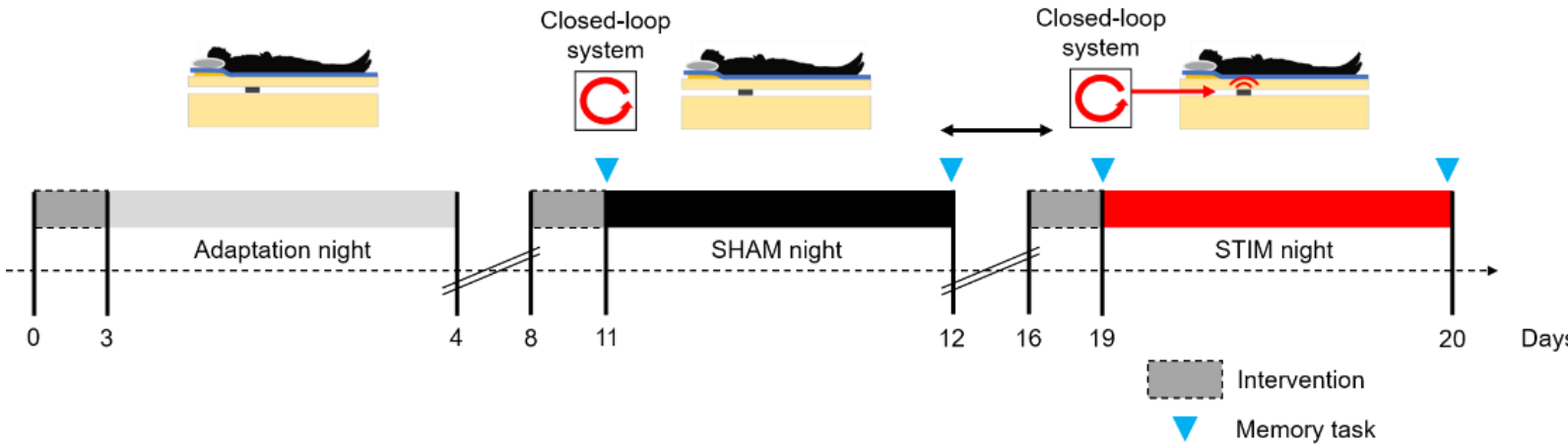


**Figure 4-1.** Study Design. Ten participants underwent one adaptation night and two experimental nights. Two experimental conditions were administered in a randomized order. During STIM night, closed-loop vibration stimulation was applied (red) and during SHAM night, closed-loop system was activated but stimulation was muted (black). During three days before each experiment, intervention was applied to the participants such as maintain regular sleep and refrain from drinking alcohol. Memory tasks were conducted in the evening and in the morning of each condition.

### 4.1.3. Heart Rate Variability & Synchronization Analysis

To evaluate the effect of closed-loop stimulation on the ANS during sleep, HRV and synchronization ratio were analyzed in each sleep stage. The HRV parameters were extracted following section 3.1.1.3. method.

Furthermore, the synchronization ratio was computed between heartbeats and stimuli. The synchronization analysis was performed using synchrogram following section 3.2.1.3. method. In this study, the threshold determinant factor ($\Delta$) was set to 3 or 4, and $T$ was set to 10 s to assess synchronization ratio in each stage epoch (30 s). Synchronization epochs were detected only under the 1:1 ratio condition for heartbeats:stimuli. The surrogate data were constructed from the SHAM condition data to check the effect of vibration stimulation on synchronization. The same rule was applied by which the −3% stimulus BPM is calculated from the previous 5 min mean HR to obtain the stimulus signal for the baseline data. Then, the synchronization ratio was computed from WASO, N1, N2, N3, and REM sleep stage and compared with between SHAM and STIM condition.

### 4.1.4. EEG Spectral Analysis

To assess the effects of closed-loop stimulation on EEG, spectral analysis was conducted in each sleep stage. Before EEG analyzing, the artifacts were detected using an automatic artifact detection method built into the open-source Fieldtrip software [125]. This software detected abnormal EEG segments based on z-score method as follow steps: 1) Calculating mean and SD of each channel over all samples, 2) Z-normalizing of each channel by subtracting its mean and dividing by the SD, 3) Averaging all channel z-values per timepoint and considering the segment where accumulated z-score is above the threshold as artifact. Segments detected to be an artifact were excluded from EEG spectral analysis. From F3 EEG channel, power spectra were calculated by Welch's modified periodogram method [126] using a Hamming window with 0.25 Hz resolution (4 s windows, 50% overlapping). Power spectra were normalized by dividing its cumulative power up to 30 Hz to account for individual variability. Mean power was computed following frequency bands: Slow wave activity (SWA, 0.5-4 Hz), theta (4-8 Hz), alpha (8-12 Hz), sigma (12-16 Hz), and beta (16-30 Hz). Above frequency bands power were extracted from WASO, N1, N2, N3, and REM sleep stage and compared the difference of band power between SHAM and STIM condition. The HRV, synchronization, and EEG spectral analysis were analyzed using MATLAB R2018b (MathWorks, Natick, MA, USA) software.

### 4.1.5. Memory Retention Test

To assess the effect of closed-loop stimulation on declarative memory, a word paired-associated learning task was conducted [65]. The task consisted of 54 semantically related Korean word-pairs and two different word lists were used for

two experimental conditions (SHAM and STIM). Participants conducted one learning phase and two recall phases in each condition (Figure 4-2). At the learning phase before sleep, participants learned the 54 word-pairs (see appendix) presented on a monitor, each for 4 s and with an inter-stimulus interval of 1 s. After the learning phase, participants conducted an immediate recall test (pre-sleep), in which participants had to type the associated word on presentation of the first word, with the word-pairs presented in random order. When the participant entered an incorrect word, the correct answer was feedbacked at the end of each trial. If the percentage of correct responses did not exceed 60%, the learning and test processes were performed again. In the morning, a delayed recall test (post-sleep) was conducted in the same manner as immediately recall phase, except that there was no feedback to the answer. Overnight memory retention was computed by the difference in the recall performance between delayed recall test (after sleep) and immediate recall test (before sleep). Statistical difference of memory retention was compared between SHAM and STIM conditions.

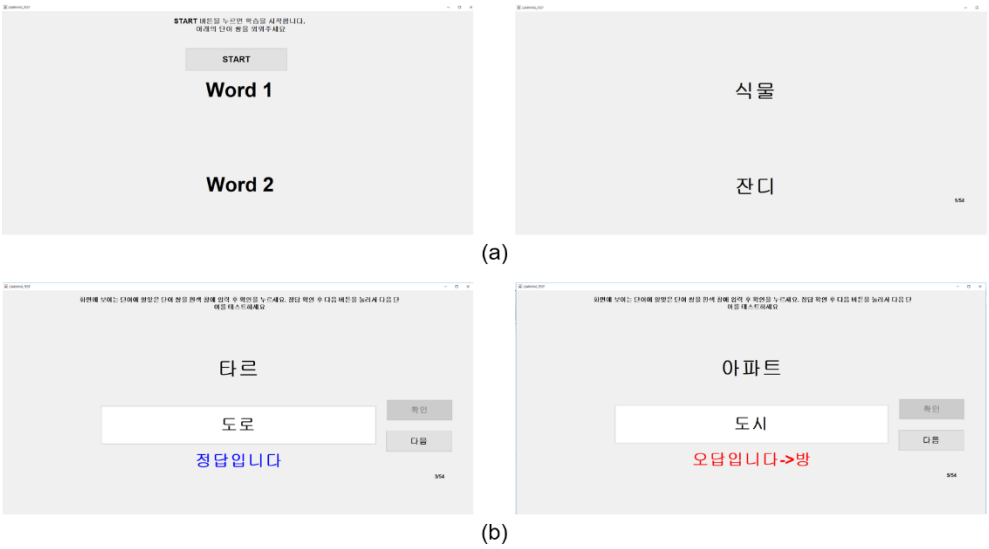


**Figure 4-2.** Example of memory task program for (a) word-pairs learning phase and (b) recall phase.

### 4.1.6. Statistical Analysis

All variables were tested for normality using the Kolmogorove-Smirnov test with a significance level of $p<0.05$. To verify the effect of the stimulation, if variables were normally distributed, a paired t-test was employed. If not, a Wilcoxon signed-rank sum test was used. A p-value of less than 0.05 was considered significant. The statistical analysis was performed using the SPSS statistics program (v. 25.0, SPSS Inc., Chicago, Illinois, USA).

## 4.2. Results

### 4.2.1. Sleep Macrostructure Results

Figure 4-3 presents the mean values of each sleep structure parameter. In sleep macrostructure analysis, there were no significant difference parameters between the SHAM and STIM conditions.

### 4.2.2. Heart Rate Variability & Synchronization Results

Table 4-1 summarizes the time- and frequency-domain HRV parameters according to each stage. There was no significant difference in the time-domain HRV parameters for the SHAM and STIM conditions. In the frequency domain parameters, the nLF under the STIM condition was significantly lower than that under the SHAM condition in N3 stage ($p<0.03$, paired t-test). In addition, the nHF parameter was significantly higher under the STIM condition than under the SHAM condition in N3 stage ($p<0.03$, paired t-test).

Furthermore, as shown in Figure 4-4, the synchronization ratio between heartbeats and stimuli in N3 stage was significantly higher under the STIM condition than the SHAM condition ($p<0.01$, paired t-test).

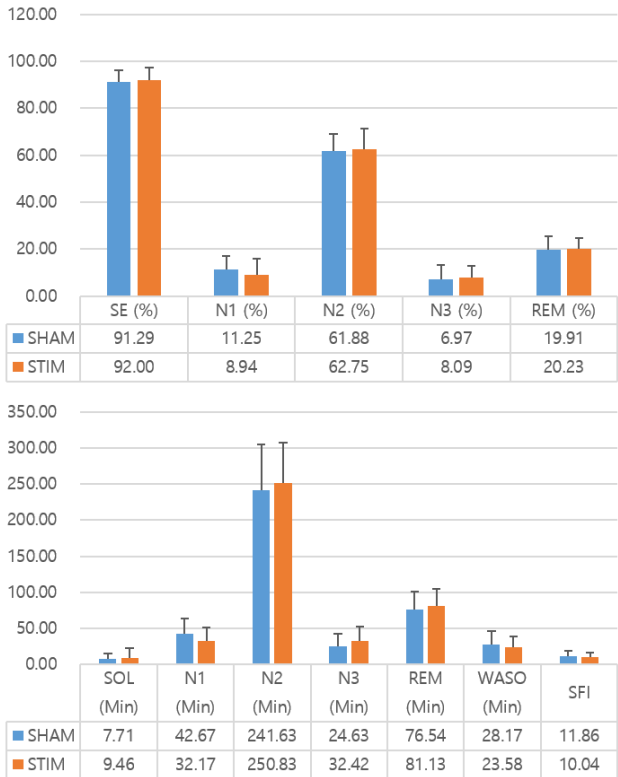


**Figure 4-3.** Effects of closed-loop stimulation on sleep macrostructure. Mean (± s.d.) sleep macrostructure parameters during the SHAM and STIM conditions. SE, sleep efficiency; SOL, sleep onset latency; WASO, wake after sleep onset; SFI, sleep fragmentation index.

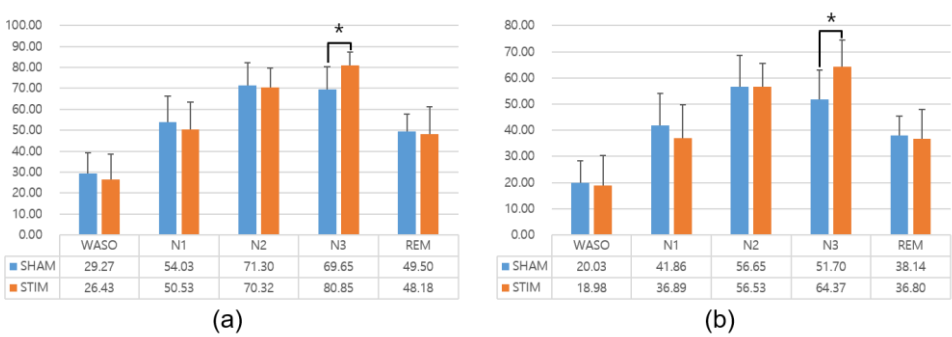


**Figure 4-4.** Effects of closed-loop stimulation on synchronization ratio in each stage. (a) Mean (± s.d.) of synchronization ratio when the threshold determinant factor (Δ) was 3, (b) Mean (± s.d.) of synchronization ratio when the threshold determinant factor (Δ) was 4. *$p<0.01$ between the SHAM and STIM conditions (paired t-test). WASO, wake after sleep onset; REM, rapid eye movement.

**Table 4-1.** Effects of closed-loop stimulation on heart rate variability
(Mean ± Standard Deviation)

| Stage & Condition /Variable | | Mean HR | pNN50 | SDNN | RMSSD | nLF | nHF | LF/HF |
|---|---|---|---|---|---|---|---|---|
| WASO | SHAM | 64.25 ±6.21 | 15.33 ±9.19 | 105.52 ±34.08 | 64.55 ±31.40 | 0.65 ±0.08 | 0.35 ±0.08 | 2.31 ±0.94 |
| | STIM | 64.08 ±5.63 | 14.44 ±8.26 | 104.77 ±35.47 | 58.46 ±27.47 | 0.65 ±0.06 | 0.35 ±0.06 | 2.23 ±0.54 |
| N1 | SHAM | 63.78 ±6.94 | 15.37 ±9.60 | 99.63 ±42.77 | 66.03 ±36.20 | 0.64 ±0.08 | 0.36 ±0.08 | 2.38 ±1.32 |
| | STIM | 63.54 ±5.76 | 15.27 ±8.63 | 102.91 ±42.39 | 62.79 ±33.12 | 0.66 ±0.08 | 0.34 ±0.08 | 2.44 ±0.66 |
| N2 | SHAM | 59.78 ±5.44 | 18.48 ±10.70 | 75.51 ±28.34 | 66.26 ±27.43 | 0.52 ±0.09 | 0.48 ±0.09 | 1.43 ±0.59 |
| | STIM | 61.20 ±7.22 | 17.17 ±10.38 | 79.05 ±35.84 | 65.59 ±33.18 | 0.56 ±0.13 | 0.44 ±0.13 | 1.86 ±1.11 |
| N3 | SHAM | 63.44 ±9.21 | 14.79 ±13.11 | 50.20 ±27.50 | 55.07 ±32.52 | **0.44 ±0.14** | **0.56 ±0.14** | 1.12 ±0.98 |
| | STIM | 61.62 ±5.82 | 17.13 ±10.26 | 47.57 ±16.49 | 56.45 ±24.69 | **0.35 ±0.14*** | **0.65 ±0.14*** | 0.71 ±0.57 |
| REM | SHAM | 64.81 ±8.13 | 12.31 ±9.14 | 82.92 ±38.14 | 59.20 ±37.57 | 0.67 ±0.11 | 0.33 ±0.11 | 2.68 ±1.31 |
| | STIM | 64.25 ±6.45 | 12.65 ±8.97 | 85.91 ±32.07 | 57.67 ±33.38 | 0.70 ±0.08 | 0.30 ±0.08 | 2.92 ±1.21 |

HR, heart rate; pNN50, percentage of successive RR intervals that differ by more than 50 ms; SDNN, standard deviation of the RR intervals; RMSSD, root mean square of the successive RR interval differences; nLF, normalized low-frequency band power; nHF, normalized high-frequency band power; LF/HF, ratio of the low-frequency power to the high-frequency power.
*$p$<0.03 between the SHAM and STIM conditions (paired t-test).

### 4.2.3. EEG Spectral Analysis & Memory Retention Results

In EEG spectral analysis, SWA and Theta frequency band power was significantly increased under the STIM condition than the SHAM condition in N3 stage ($p<0.03$, Wilcoxon rank-sum test, Figure 4-5(a)). In N2 stage, Beta frequency band power under the STIM condition was significantly lower than the SHAM condition ($p<0.01$, Wilcoxon rank-sum test). Except for the above cases, there were no significant differences in frequency band relative power between the SHAM and STIM conditions in the other sleep stages.

Figure 4-5(b) presents the memory retention in the SHAM and the STIM conditions. As you can see, memory retention was significantly increased under the STIM condition than under the SHAM condition ($p<0.05$, paired t-test).


**Figure 4-5.** Effects of closed-loop stimulation on EEG spectral frequency band in N3 sleep stage and memory retention. (a) Mean (± s.d.) of spectral relative power in each frequency band, (b) Mean (± s.d.) of memory retention between the SHAM and STIM conditions. *$p<0.05$ between the SHAM and STIM conditions (paired t-test). **$p<0.03$ between the SHAM and STIM conditions (Wilcoxon rank-sum test). SWA, slow wave activity.

## 4.3. Discussion

In this study, the effects of closed-loop vibration stimulation on sleep and memory were investigated. Vibration stimulus, which updated every 5 min based on previous mean HR, was applied continuously during whole night sleep. In previous study [124], it was confirmed that closed-loop vibration stimulation influencing heart rhythm and deriving ANS stabilization. Furthermore, the smaller detuning percent, which external stimulus BPM is closer to the HR, showed a larger HR modulation. Here, −3% stimulus BPM, calculated on the basis of the mean HR computed over the previous 5 min, was applied and the effects on sleep were confirmed. Although there was no significant change in sleep macrostructure, stimulation improved memory retention and N3 sleep stage quality in a microstructure perspective.

First, in sleep macrostructure analysis, there were no significant changed parameters between the SHAM and STIM conditions. Given that participants were healthy and already had a good sleep structure, it is hypothesized that the sleep architecture may have reached a ceiling effect, such that vibration stimulation could not enhance sleep structure. In previous studies that induced slow oscillations by applying closed-loop auditory stimuli, as in this study, there was no change in sleep structure and significant differences only in memory retention and EEG parameters [66], [67], [123]. Furthermore, stimulation effects were tested just one-night sleep and to the participant who has a good sleep structure. Under these conditions, there is a limitation to change sleep structure, so it is necessary to apply stimulation for several days and confirm the effect. In addition, to clarify the effects of the closed-loop stimulation system on sleep structure, there needs an additional experiment in

people who have a sleep fragmentation or have low sleep efficiencies, such as elderly people or insomnia patients.

Second, the HRV parameters were analyzed in each sleep stage. In the N3 sleep stage, the nHF parameter, which represents the parasympathetic activity [113], significantly increased under the STIM condition compared with the SHAM condition, and the nLF parameter, which represents the sympathovagal balance [113], significantly decreased under the STIM condition compared with the SHAM condition. In the other sleep stages except for the N3 sleep stage, there were no HRV parameters that showed a significant difference between the two conditions. From these results, it is confirmed that stimulation derived stabilization of ANS, specifically in the N3 sleep stage.

To demonstrate the vibration stimulus effects on the heartbeat, phase synchronization analysis was conducted in each sleep stage. The synchronization ratio was significantly increased only in the N3 sleep stage during the STIM condition compared with the SHAM condition. There is one possible reason why the stimulation effected only in the N3 sleep stage. Physiological heart rhythm variability is the most stable in the N3 stage compared to the other sleep stages. Thus, when a constant stimulus BPM is applied for 5 minutes, in N3 sleep stage, the difference between the heartbeat and the stimulation BPM falls within the range of 3%, while the other sleep stages have greater variability and thus the difference between the heartbeat and stimulation BPM could out of the 3% range. As for this reason, synchronization may appear more effective in the N3 sleep stage, consequently, the synchronization ratio was significantly increased.

The SWA has been studied that it increases at the recovery state after sleep

deprivation [127] and relates to the cortical maturation [128]. Furthermore, SWA is also an important criterion when scoring N3 sleep stages [21] and it is known to associate with the overnight memory consolidation [129]. In EEG spectral analysis, the spectral relative power of the SWA in the N3 sleep stage was significantly increased during the STIM condition compared with the SHAM condition. Also, the relative spectral power of the theta frequency band was significantly increased under the STIM condition. The previous study suggested that the encoding of new information is reflected by theta oscillations [130]. From the results of the EEG spectral analysis, it was expected that the stimulus affected the EEG change and the memory also changed. In effect, during the STIM condition, memory retention was significantly increased compared with the SHAM condition.

Taken together, the present findings demonstrate that the closed-loop stimulation during a night sleep promotes N3 sleep stage quality and memory retention. Although vibration stimulation was not induced at a specific phase of the slow oscillations like previous studies [66], [67], [123], its continuous vibration stimulus, lower than 1 Hz might have strengthened the coupling between heart rhythm and cortical oscillations, resulted in the changes of HRV and EEG spectral relative power. Because the somatosensory system sends direct inputs to the thalamus (Figure 4-6(a)), the vibration stimulus might have influenced neural activity within thalamocortical networks. The correlation between the change (STIM-SHAM) of synchronization ratio during N3 and the change of memory retention showed a significant positive correlation as shown in Figure 4-6(b) (Pearson's correlation coefficient = 0.752, $p < 0.01$). This result suggested the possibility that external stimulation modulated heart rhythm and influenced the

change of memory retention. Further studies of the heart-brain-sleep connection and interaction are needed to better understand the effects of the stimulation on sleep.

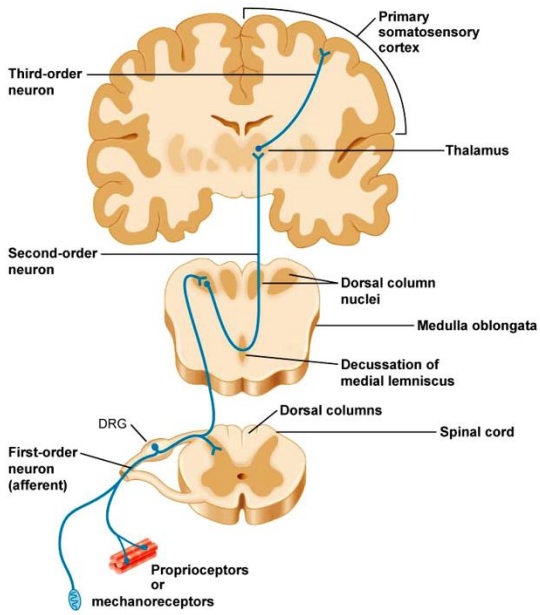


(a)

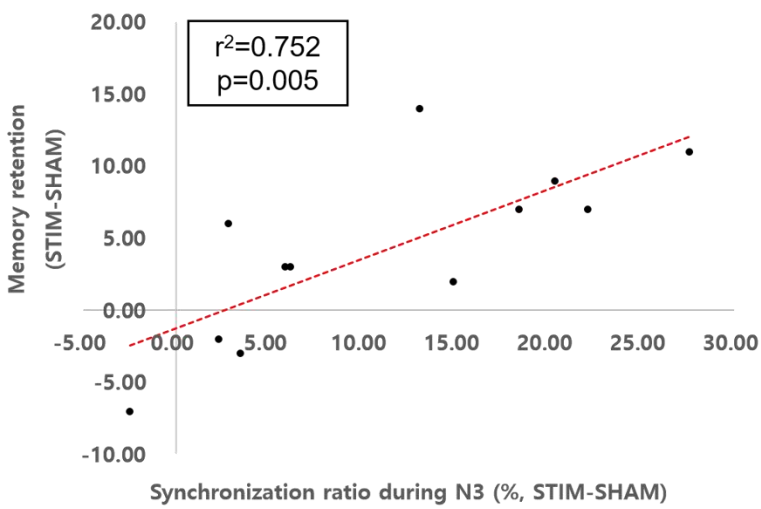


(b)

**Figure 4-6.** (a) Somatosensory pathway (*Source*: Google image), (b) Scatter plot showing significant correlation (p = 0.005) between the change (STIM minus SHAM) in synchronization ratio during N3 and change in memory retention.

# 5
# Conclusion

In this thesis, a bidirectional-LSTM model for classifying four sleep stages using unconstrained signals recorded by a PVDF sensor was developed. The developed LSTM model uses autonomic and movement information derived from BCG signals for scoring the sleep stage, and this model could learn sequential patterns of sleep. As a result, the proposed LSTM model provided competitive results as compared with other machine learning methods and previous studies. As this model uses parameters extracted from the BCG signal, if reliability is ensured that the same features can be extracted from other modalities, the proposed LSTM model could be applied to alternative signals such as ECG or PPG. By pre-training and fine-tuning, this model could become applicable to wearable devices that provide ANS-related information such as watch-type or patch-type devices. The study provides a solution for long-term sleep monitoring at home, which will have a positive impact on healthcare. Besides providing useful information on one's health, it can be used to observe the improvement of patient's sleep quality after treatments.

In addition, a novel and feasible closed-loop stimulation system was developed.

The closed-loop vibration stimulation systems influenced the heart rhythm and stabilized the ANS. A small detuning percent modulated the heart rhythm, implying that an external stimulus BPM closer to the HR had a larger effect on HR modulation. The closed-loop vibration-stimulation system was most effective in stabilizing the heart rhythm compared with methods such as open-loop vibration, auditory, and current stimulation. Its effects on sleep and memory were investigated during the night sleep and results show that it improved N3 sleep stage quality and memory retention. This suggests that closed-loop vibration stimulus during sleep could be therapeutic for cardiovascular and mental health. Though various stimulation methods for sleep enhancement exist, this system is innovative, as it is unobtrusive and practical for long-term use. This study will be a new strategy for sleep enhancement.

# 6

# References


[1] J. Krueger and F. Obal Jr., “Sleep function,” *Front. Biosci.*, vol. 8, no. 3, pp. 511–519, 2003.

[2] F. Crick and G. Mitchison, “The function of dream sleep,” *Nature*, pp. 111–114, 1983.

[3] G. Tononi and C. Cirelli, “Sleep function and synaptic homeostasis,” *Sleep Med. Rev.*, vol. 10, no. 1, pp. 49–62, 2006.

[4] J. M. Krueger *et al.*, “Sleep as a fundamental property of neuronal assemblies,” *Nat. Rev. Neurosci.*, vol. 9, no. 12, pp. 910–919, 2008.

[5] J. M. Siegel, “Clues to the functions of mammalian sleep,” *Nature*, vol. 437, no. 7063, pp. 1264–1271, 2005.

[6] J. M. Krueger and F. Obal Jr., “A neuronal group theory of sleep function,” *J. Sleep Res.*, pp. 63–69, 1993.

[7] M. P. Walker *et al.*, “Cognitive flexibility across the sleep-wake cycle: REM-sleep enhancement of anagram problem solving,” *Cogn. Brain Res.*, vol. 14, no. 3, pp. 317–324, 2002.

[8] U. Wagner *et al.*, “Sleep inspires insight,” *Nature*, vol. 427, no. January, pp. 21–24, 2004.

[9] M. Massimini *et al.*, “Triggering sleep slow waves by transcranial magnetic stimulation,” *Proc. Natl. Acad. Sci.*, vol. 104, no. 20, pp. 8496–8501, 2007.

[10] M. P. Barham *et al.*, “Transcranial electrical stimulation during sleep enhances declarative (but not procedural) memory consolidation: Evidence from a meta-analysis,” *Neurosci. Biobehav. Rev.*, vol. 63, pp. 65–77, 2016.

[11] A. Sadeh, “The role and validity of actigraphy in sleep medicine: An update,” *Sleep Med. Rev.*, vol. 15, no. 4, pp. 259–267, 2011.

[12] J. D. F. Dinges *et al.*, “Cumulative Sleepiness, Mood Disturbance, and Psychomotor Vigilance Performance Decrements During a Week of Sleep Restricted to 4–5 Hours per Night,” *Sleep*, vol. 20, no. 4, pp. 267–277, 1997.

[13] G. Curcio *et al.*, “Sleep loss, learning capacity and academic performance,” *Sleep Med. Rev.*, vol. 10, no. 5, pp. 323–337, 2006.

[14] J. S. Durmer *et al.*, “Neurocognitive consequences of sleep deprivation,” *Semin. Neurol.*, vol. 25, no. Yolen 1987, p. 1996, 2000.

[15] W. M. A. Van Leeuwen *et al.*, “Sleep restriction increases the risk of developing cardiovascular diseases by augmenting proinflammatory responses through IL-17 and CRP,” *PLoS One*, vol. 4, no. 2, 2009.

[16] B. Faraut *et al.*, “Immune, inflammatory and cardiovascular consequences of sleep restriction and recovery,” *Sleep Med. Rev.*, vol. 16, no. 2, pp. 137–149, 2012.

[17] J. M. Mullington *et al.*, “Cardiovascular, Inflammatory, and Metabolic Consequences of Sleep Deprivation,” *Prog. Cardiovasc. Dis.*, vol. 51, no. 4, pp. 294–302, 2009.

[18] M. A. Cappuccio *et al.*, “Meta-Analysis of Short Sleep Duration and Obesity in Children and Adults,” *Sleep*, vol. 31, no. 5, pp. 619–626, 2008.

[19] J. E. Gangwisch *et al.*, “Inadequate sleep as a risk factor for obesity: analyses of the NHANES I,” pp. 10–12, 1992.

[20] A. Rechtschaffen, “A manual of standardized terminology, techniques and scoring

system for sleep stages of human subjects," *Natl. Institutes Heal.*, 1968.

[21] R. B. Berry *et al.*, "The AASM manual for the scoring of sleep and associated events: rules, terminology and technical specifications, Version 2.0," *Am. Acad. Sleep Med.*, 2012.

[22] X. Omlin, "The Effect of Vestibular Stimulation on Sleep and Cardio-Respiratory Functions," PhD Thesis, ETH Zurich, 2015.

[23] T. Penzel *et al.*, "Inter-scorer Reliability between Sleep Centers Can Teach Us What to Improve in the Scoring Rules," *J. Clin. Sleep Med.*, vol. 9, no. 1, pp. 3–5, 2013.

[24] M. Younes *et al.*, "Reliability of the American Academy of Sleep Medicine Rules for Assessing Sleep Depth in Clinical Practice," *J. Clin. Sleep Med.*, vol. 14, no. 2, pp. 205–213, 2018.

[25] R. S. Rosenberg and S. Van Hout, "The American Academy of Sleep Medicine inter-scorer reliability program: Respiratory events," *J. Clin. Sleep Med.*, vol. 10, no. 4, pp. 447–454, 2014.

[26] K. S. Park and S. H. Choi, "Smart technologies toward sleep monitoring at home," *Biomed. Eng. Lett.*, no. 0123456789, 2019.

[27] M. Marino *et al.*, "Measuring Sleep: Accuracy, Sensitivity, and Specificity of Wrist Actigraphy Compared to Polysomnography," *Sleep*, vol. 36, no. 11, pp. 1747–1755, 2013.

[28] P. T. Ko *et al.*, "Consumer sleep technologies: A review of the landscape," *J. Clin. Sleep Med.*, vol. 11, no. 12, pp. 1455–1461, 2015.

[29] C. C. Yang and Y. L. Hsu, "A review of accelerometry-based wearable motion detectors for physical activity monitoring," *Sensors*, vol. 10, no. 8, pp. 7772–7788, 2010.

[30] E. Fino and M. Mazzetti, "Monitoring healthy and disturbed sleep through smartphone applications: a review of experimental evidence," *Sleep Breath.*, vol.

23, no. 1, pp. 13–24, 2019.

[31] B. H. Choi *et al.*, “Non-constraining sleep/wake monitoring system using bed actigraphy,” *Med. Biol. Eng. Comput.*, vol. 45, no. 1, pp. 107–114, 2007.

[32] S. H. Hwang *et al.*, “Unconstrained sleep stage estimation based on respiratory dynamics and body movement,” *Methods Inf. Med.*, vol. 55, no. 6, pp. 545–555, 2016.

[33] P. de Chazal *et al.*, “Assessment of sleep/wake patterns using a non-contact biomotion sensor,” *2008 30th Annu. Int. Conf. IEEE Eng. Med. Biol. Soc.*, pp. 514–517, 2008.

[34] E. O’Hare *et al.*, “A comparison of radio-frequency biomotion sensors and actigraphy versus polysomnography for the assessment of sleep in normal subjects,” *Sleep Breath.*, vol. 19, no. 1, pp. 91–98, 2015.

[35] W.-H. Liao and C.-M. Yang, “Video-based activity and movement pattern analysis in overnight sleep studies,” *2008 19th Int. Conf. Pattern Recognit.*, pp. 1–4, 2008.

[36] S. Sathyanarayana *et al.*, “Vision-based patient monitoring: a comprehensive review of algorithms and technologies,” *J. Ambient Intell. Humaniz. Comput.*, vol. 9, no. 2, pp. 225–251, 2018.

[37] O. Tsinalis *et al.*, “Automatic Sleep Stage Scoring with Single-Channel EEG Using Convolutional Neural Networks,” *Prepr. arXiv*, p. 12, 2016.

[38] L. Fraiwan *et al.*, “Automated sleep stage identification system based on time-frequency analysis of a single EEG channel and random forest classifier,” *Comput. Methods Programs Biomed.*, vol. 108, no. 1, pp. 10–19, 2012.

[39] R. J. Cole *et al.*, “Automatic sleep/wake identification from wrist activity,” *Sleep*, vol. 15, no. 5, pp. 461–469, 1992.

[40] J. Trinder *et al.*, “Autonomic activity during human sleep as a function of time and sleep stage,” *J. sleep*, vol. 10, no. 4, pp. 253–264, 2001.

[41] Z. Shinar *et al.*, “Autonomic changes during wake-sleep transition: A heart rate

variability based approach," *Autonomic Neuroscience: Basic and Clinical*, vol. 130, no. 1–2. pp. 17–27, 2006.

[42] I. M. Voronin and E. V. Biryukova, "Heart rate variability in healthy humans during night sleep," *Hum. Physiol.*, vol. 32, no. 3, pp. 258–263, 2006.

[43] A. Baharav *et al.*, "Fluctuations in autonomic nervous activity during sleep displayed by power spectrum analysis of heart rate variability," *Neurology*, vol. 45, no. 6, pp. 1183–1187, 1995.

[44] V. K. Somers *et al.*, "Sympathetic-Nerve Activity during Sleep in Normal Subjects," *N. Engl. J. Med.*, 1993.

[45] H. Yoon *et al.*, "Slow-Wave Sleep Estimation for Healthy Subjects and OSA Patients Using R-R Intervals," *IEEE J. Biomed. Heal. Informatics*, vol. 22, no. 1, pp. 119–128, 2018.

[46] M. Xiao *et al.*, "Sleep stages classification based on heart rate variability and random forest," *Biomed. Signal Process. Control*, vol. 8, no. 6, pp. 624–633, 2013.

[47] B. Yilmaz *et al.*, "Sleep stage and obstructive apneaic epoch classification using single-lead ECG," *Biomed. Eng. Online*, vol. 9, pp. 1–14, 2010.

[48] H. Yoon *et al.*, "REM sleep estimation based on autonomic dynamics using R-R intervals.," *Physiol. Meas.*, vol. 38, no. 4, pp. 631–651, 2017.

[49] J. Hedner *et al.*, "Sleep staging based on autonomic signals: a multi-center validation study.," *J. Clin. Sleep Med.*, vol. 7, no. 3, pp. 301–6, Jun. 2011.

[50] M. Bresler *et al.*, "Differentiating between light and deep sleep stages using an ambulatory device based on peripheral arterial tonometry.," *Physiol. Meas.*, vol. 29, no. 5, pp. 571–84, May 2008.

[51] S. Herscovici *et al.*, "Detecting REM sleep from the finger: An automatic REM sleep algorithm based on peripheral arterial tone (PAT) and actigraphy," *Physiol. Meas.*, vol. 28, no. 2, pp. 129–140, 2007.

[52] P. Fonseca *et al.*, "Validation of photoplethysmography-based sleep staging

compared with polysomnography in healthy middle-aged adults," *Sleep*, vol. 40, no. 7, 2017.

[53] Y. LeCun *et al.*, "Deep learning," *Nature*, vol. 521, no. 7553, pp. 436–444, 2015.

[54] H. Phan *et al.*, "Joint Classification and Prediction CNN Framework for Automatic Sleep Stage Classification," *IEEE Trans. Biomed. Eng.*, vol. 66, no. 5, pp. 1285–1296, 2019.

[55] J. B. Stephansen *et al.*, "Neural network analysis of sleep stages enables efficient diagnosis of narcolepsy," *Nat. Commun.*, pp. 1–15, 2018.

[56] H. Dong *et al.*, "Mixed Neural Network Approach for Temporal Sleep Stage Classification," *IEEE Trans. Neural Syst. Rehabil. Eng.*, vol. 26, no. 2, pp. 324–333, 2018.

[57] A. Supratak *et al.*, "DeepSleepNet: A model for automatic sleep stage scoring based on raw single-channel EEG," *IEEE Trans. Neural Syst. Rehabil. Eng.*, vol. 25, no. 11, pp. 1998–2008, 2017.

[58] K. Kräuchi *et al.*, "Physiology: warm feet promote the rapid onset of sleep," *Nature*, vol. 5477, no. 1991, pp. 0–2, 1999.

[59] G. De Niet *et al.*, "Music-assisted relaxation to improve sleep quality: Meta-analysis," *J. Adv. Nurs.*, vol. 65, no. 7, pp. 1356–1364, 2009.

[60] L. Bayer *et al.*, "Rocking synchronizes brain waves during a short nap," *Curbio*, vol. 21, no. 12, pp. R461–R462, 2011.

[61] R. Velutti, "Interactions between sleep and sensory physiology," *J. Sleep Res.*, vol. 6, no. 2, pp. 61–77, 1997.

[62] L. Cordero *et al.*, "Effects of Vestibular Stimulation on Sleep States in Premature Infants," *American Journal of Perinatology*, vol. 3, no. 4. pp. 319–324, 1986.

[63] A. A. Perrault *et al.*, "Whole-Night Continuous Rocking Entrains Spontaneous Neural Oscillations with Benefits for Sleep and Memory," *Curr. Biol.*, vol. 29, no. 3, pp. 402-411.e3, 2019.

[64] G. Bellesi *et al.*, “Enhancement of sleep slow waves: underlying mechanisms and practical consequences,” *Front. Syst. Neurosci.*, vol. 8, 2014.

[65] L. Marshall *et al.*, “Boosting slow oscillations during sleep potentiates memory.,” *Nature*, vol. 444, no. November, pp. 610–613, 2006.

[66] H. V. V Ngo *et al.*, “Auditory closed-loop stimulation of the sleep slow oscillation enhances memory,” *Neuron*, vol. 78, pp. 545–553, 2013.

[67] R. Lehmann *et al.*, “Auditory closed-loop stimulation of EEG slow oscillations strengthens sleep and signs of its immune-supportive function,” *Nat. Commun.*, vol. 8, no. 1, 2017.

[68] J. L. Ong *et al.*, “Auditory stimulation of sleep slow oscillations modulates subsequent memory encoding through altered hippocampal function,” *Sleep*, vol. 41, no. 5, pp. 1–11, 2018.

[69] R. F. Helfrich *et al.*, “Entrainment of brain oscillations by transcranial alternating current stimulation,” *Curr. Biol.*, vol. 24, no. 3, pp. 333–339, 2014.

[70] E. Debellemaniere *et al.*, “Performance of an Ambulatory Dry-EEG Device for Auditory Closed-Loop Stimulation of Sleep Slow Oscillations in the Home Environment,” *Front. Hum. Neurosci.*, vol. 12, no. March, pp. 1–15, 2018.

[71] A. Pikovsky *et al.*, *Synchronization: A Universal Concept in Nonlinear Science*, vol. 70, no. 6. 2002.

[72] J. Buck and E. Buck, “Mechanism of rhythmic synchronous flashing of fireflies,” *Science (80-. ).*, vol. 159, no. 3821, pp. 1319–1327, 1968.

[73] T. J. Walker, “Acoustic synchrony: Two mechanisms in the snowy tree cricket,” *Science (80-. ).*, vol. 166, no. 3907, pp. 891–894, 1969.

[74] A. Angelone and Norman A. Coulter JR, “Respiratory sinus arrhythmia a frequency dependent phenomenon,” *J. Appl. Physiol.*, pp. 479–482, 1964.

[75] G. Brandenberger *et al.*, “Inverse coupling between ultradian oscillations in delta wave activity and heart rate variability during sleep,” *Clin. Neurophysiol.*, vol. 112,

no. 6, pp. 992–996, 2001.

[76] F. Jurysta *et al.*, “A study of the dynamic interactions between sleep EEG and heart rate variability in healthy young men,” *Clin. Neurophysiol.*, vol. 114, no. 11, pp. 2146–2155, 2003.

[77] V. Novak *et al.*, “Cardiolocomotor coupling in young and elderly people,” *Journals Gerontol. - Ser. A Biol. Sci. Med. Sci.*, vol. 62, no. 1, pp. 86–92, 2007.

[78] K. Nomura *et al.*, “Analysing entrainment of cardiac and locomotor rhythms in humans using the surrogate data technique,” *Eur. J. Appl. Physiol.*, vol. 84, no. 5, pp. 373–378, 2001.

[79] C. A. Czeisler *et al.*, “Bright light resets the human circadian pacemaker independent of the timing of the sleep-wake cycle,” *Science (80-. ).*, vol. 233, no. 4764, pp. 667–671, 1986.

[80] R. Y. Moore, “A clock for the ages,” *Science (80-. ).*, pp. 2102–2103, 1999.

[81] M. K. McClinton, “Menstrual synchrony and suppression.,” *Nature*, vol. 229, pp. 244–245, 1971.

[82] P. Van Leeuwen *et al.*, “Influence of paced maternal breathing on fetal-maternal heart rate coordination,” *Proceedings of the National Academy of Sciences*, vol. 106, no. 33. pp. 13661–13666, 2009.

[83] D. Grimaldi *et al.*, “Strengthening sleep-autonomic interaction via acoustic enhancement of slow oscillations,” *Sleep*, vol. 42, no. 5, 2019.

[84] G. V. Anishchenko *et al.*, “Entrainment Between Heart Rate and Weak Noninvasive Forcing,” *Int. J. Bifurc. Chaos*, vol. 10, no. 10, pp. 2339–2348, 2000.

[85] H. Yoon *et al.*, “Human heart rhythms synchronize while co-sleeping,” *Front. Physiol.*, vol. 10, p. 190, 2019.

[86] C. S. Kim *et al.*, “Ballistocardiogram: Mechanism and Potential for Unobtrusive Cardiovascular Health Monitoring,” *Sci. Rep.*, vol. 6, pp. 1–6, 2016.

[87] G. Roopa Manjunatha *et al.*, “Polyvinylidene fluoride film based nasal sensor to

monitor human respiration pattern: An initial clinical study," *J. Clin. Monit. Comput.*, vol. 27, no. 6, pp. 647–657, 2013.

[88] S. Choi and Z. Jiang, "A novel wearable sensor device with conductive fabric and PVDF film for monitoring cardiorespiratory signals," *Sensors Actuators, A Phys.*, vol. 128, no. 2, pp. 317–326, 2006.

[89] F. Wang *et al.*, "Development of a PVDF Piezopolymer Sensor for Unconstrained In-sleep Cardiorespiratory Monitoring," *J. Intell. Mater. Syst. Struct.*, vol. 14, no. March, pp. 1–7, 2003.

[90] Y. Y. Chiu *et al.*, "Development of a piezoelectric polyvinylidene fluoride polymer-based sensor patch for simultaneous heartbeat and respiration monitoring," *Sensors Actuators, A Phys.*, vol. 189, pp. 45–48, 2013.

[91] H. J. Baek *et al.*, "A Smart Health Monitoring Chair for Nonintrusive Measurement of Biological Signals," vol. 16, no. 1, pp. 150–158, 2012.

[92] M. H. Jones *et al.*, "Reliable respiratory rate estimation from a bed pressure array," *Annu. Int. Conf. IEEE Eng. Med. Biol. - Proc.*, pp. 6410–6413, 2006.

[93] A. Savitzky and M. J. E. Golay, "Smoothing and Differentiation of Data by Simplified Least Squares Procedures," *Anal. Chem.*, vol. 36, no. 8, pp. 1627–1639, 1964.

[94] N. Srivastava *et al.*, "Dropout: A Simple Way to Prevent Neural Networks from Overfitting," *J. Mach. Learn. Res.*, vol. 15, pp. 1929–1958, 2014.

[95] D. P. Kingma and J. Ba, "Adam: A Method for Stochastic Optimization," *arXiv Prepr. arXiv1412.6980*, pp. 1–15, 2014.

[96] A. Malafeev *et al.*, "Automatic Human Sleep Stage Scoring Using Deep Neural Networks," *Front. Neurosci.*, vol. 12, no. November, pp. 1–15, 2018.

[97] F. Chollet, "Keras (2015)," *URL http//keras. io*, 2017.

[98] M. K. Martín Abadi *et al.* "TensorFlow: A System for Large-Scale Machine Learning," *Proc. 12th USENIX Conf. Oper. Syst. Des. Implement.*, p. 44, 2005.

[99] A. J. Viera and J. M. Garrett, “Understanding interobserver agreement: the kappa statistic,” *Fam. Med.*, no. May, pp. 360–363, 2005.

[100] J. M. Keller and M. R. Gray, “A Fuzzy K-Nearest Neighbor Algorithm,” *IEEE Trans. Syst. Man Cybern.*, vol. SMC-15, no. 4, pp. 580–585, 1985.

[101] C. Cortes and V. Vapni, “Support-Vector Networks,” *IEEE Expert*, vol. 7, no. 5, pp. 63–72, 1995.

[102] S. Mikat *et al.*, “Fisher discriminant analysis with kernels,” *Ieee*, pp. 41–48, 1999.

[103] S. R. Safavian and D. Landgrebe, “A Survey of Decision Tree Classifier Methodology,” *IEEE Trans. Syst. Man Cybern.*, vol. 21, no. 3, pp. 660–674, 1991.

[104] L. Breiman, “Random forests,” *Mach. Learn.*, pp. 5–32, 2001.

[105] F. Pedregosa *et al.*, “Scikit-learn: Machine Learning in python,” *J. Mach. Learn. Res.*, 2011.

[106] N. J. Douglas *et al.*, “Respiration during sleep,” pp. 840–844, 1982.

[107] V. Malik *et al.*, “Respiratory physiology during sleep,” *Sleep Medicine Clinics*. 2012.

[108] P. Fonseca *et al.*, “Sleep stage classification with ECG and respiratory effort,” *Physiol. Meas.*, vol. 36, no. 10, pp. 2027–2040, 2015.

[109] S. M. Isa *et al.*, “Kernel Dimensionality Reduction on Sleep Stage Classification using ECG Signal,” *Int. J. Comput. Sci. Issues*, vol. 8, no. 4, pp. 115–123, 2011.

[110] H. Yoon *et al.*, “Wakefulness evaluation during sleep for healthy subjects and OSA patients using a patch-type device,” *Comput. Methods Programs Biomed.*, vol. 155, pp. 127–138, 2018.

[111] M. Schuster and K. K. Paliwal, “Bidirectional Recurrent Neural Networks,” *IEEE Trans. signal Process.*, vol. 45, no. 11, p. 6757, 1997.

[112] S. H. Hwang *et al.*, “Unconstrained sleep stage estimation based on respiratory dynamics and body movement,” *Methods Inf. Med.*, vol. 55, no. 6, pp. 545–555, 2016.

[113] S. D. Camm AJ *et al.*, "Heart rate variability: standards of measurement, physiological interpretation and clinical use. Task Force of the European Society of Cardiology and the North American Society of Pacing and Electrophysiology," *Circulation*, vol. 93, pp. 1043–1065, 1996.

[114] B. H. Choi *et al.*, "Slow-wave sleep estimation on a load-cell-installed bed: A non-constrained method," *Physiol. Meas.*, vol. 30, no. 11, pp. 1163–1170, 2009.

[115] H. Beyramienanlou and N. Lotfivand, "Shannon's Energy Based Algorithm in ECG Signal Processing," *Comput. Math. Methods Med.*, vol. 2017, 2017.

[116] R. P. Bartsch *et al.*, "Phase transitions in physiologic coupling," *Proc. Natl. Acad. Sci.*, vol. 109, no. 26, pp. 10181–10186, 2012.

[117] G. Schäfer *et al.*, "Heartbeat synchronized with ventilation," *Nature*, vol. 392, no. 6673, pp. 239–240, 1998.

[118] E. Toledo *et al.*, "Does synchronization reflect a true interaction in the cardiorespiratory system?," *Med. Eng. Phys.*, vol. 24, no. 1, pp. 45–52, 2002.

[119] J. W. Antony and K. A. Paller, "Using oscillating sounds to manipulate sleep spindles," *Sleep*, vol. 40, no. 3, 2017.

[120] S. Woodward *et al.*, "Effects of otolithic vestibular stimulation on sleep," *Sleep*, vol. 13, no. 6, pp. 533–537, 1990.

[121] A. D. Krystal *et al.*, "The effect of vestibular stimulation in a four-hour sleep phase advance model of transient insomnia," *J. Clin. Sleep Med.*, vol. 6, no. 4, pp. 315–321, 2010.

[122] M. A. Carskadon and W. C. Dement, "Normal human sleep: an overview," in *Principles and Practice of Sleep Medicine*, 2005, pp. 13–23.

[123] J. L. Ong *et al.*, "Auditory stimulation of sleep slow oscillations modulates subsequent memory encoding through altered hippocampal function," *Sleep*, vol. 41, no. 5, pp. 1–11, 2018.

[124] S. H. Choi *et al.*, "Effect of Closed-Loop Vibration Stimulation on Heart Rhythm

during Naps," *Sensors*, 2019.

[125] R. Oostenveld *et al.*, "FieldTrip: Open source software for advanced analysis of MEG, EEG, and invasive electrophysiological data," *Comput. Intell. Neurosci.*, vol. 2011, 2011.

[126] P. Welch, "The Use of Fast Fourier Transform for the Estimation of Power Spectra: A Method Based on Time Aver. aging Over Short, Modified Periodograms," *IEEE Trans. audio Electroacoust.*, vol. 15, no. 2, pp. 70–73, 1967.

[127] D. Dijk *et al.*, "Dynamics of electroencephalographic sleep spindles and slow wave activity in men : effect of sleep deprivation," vol. 19, no. 41, pp. 190–199, 1993.

[128] A. Buchmann *et al.*, "EEG sleep slow-wave activity as a mirror of cortical maturation," *Cereb. Cortex*, vol. 21, no. 3, pp. 607–615, 2011.

[129] J. Holz *et al.*, "EEG sigma and slow-wave activity during NREM sleep correlate with overnight declarative and procedural memory consolidation," *Journal of Sleep Research*, vol. 21, no. 6. pp. 612–619, 2012.

[130] W. Klimesch, "EEG alpha and theta oscillations reflect cognitive and memory performance: a review and analysis," *Brain Res. Rev.*, vol. 29, no. 2–3, pp. 169–195, 1999.

# Appendix
# Korean word lists

| | List 1 | |
|---|---|---|
| 1 | 행사 | 축제 |
| 2 | 조각 | 구조 |
| 3 | 신념 | 단념 |
| 4 | 지배자 | 명령 |
| 5 | 거리 | 덤불 |
| 6 | 진술 | 증인 |
| 7 | 폭동 | 방패 |
| 8 | 업무 | 근무 |
| 9 | 기차 | 역 |
| 10 | 교량 | 물살 |
| 11 | 협약 | 조약 |
| 12 | 공장 | 생산 |
| 13 | 기계 | 사슬 |
| 14 | 함대 | 갑판 |
| 15 | 정원 | 장미 |
| 16 | 생각 | 말 |
| 17 | 관절 | 무릎 |
| 18 | 얼굴 | 가면 |
| 19 | 곡물 | 보리 |
| 20 | 빙하 | 곰 |
| 21 | 단체 | 사람 |
| 22 | 군대 | 보병대 |
| 23 | 노트 | 표시 |
| 24 | 감염 | 고통 |
| 25 | 악기 | 오보에 |
| 26 | 교회 | 종 |
| 27 | 화가 | 캔버스 |
| 28 | 벽 | 난간 |
| 29 | 가구 | 등받이 |
| 30 | 음악 | 악보 |
| 31 | 농부 | 계약 |
| 32 | 식물 | 잔디 |
| 33 | 우편 | 자전거 |
| 34 | 여행 | 대륙 |
| 35 | 파충류 | 도마뱀 |
| 36 | 연기 | 표현 |
| 37 | 배 | 부두 |
| 38 | 학교 | 관재 |
| 39 | 펜 | 뚜껑 |
| 40 | 의자 | 다리 |
| 41 | 이론 | 실습 |
| 42 | 동물 | 오소리 |
| 43 | 열대 | 접종 |
| 44 | 저승 | 죽음 |
| 45 | 부상 | 딱지 |
| 46 | 새 | 발톱 |
| 47 | 방직공 | 빗 |
| 48 | 광고 | 기둥 |
| 49 | 아파트 | 방 |
| 50 | 제동 | 회전 |
| 51 | 축하 | 맥주 |
| 52 | 거인 | 걸음 |
| 53 | 스포츠 | 시간 |
| 54 | 도로 | 타르 |

| | List 2 | |
|---|---|---|
| 1 | 곤충 | 애벌레 |
| 2 | 바다 | 조류 |
| 3 | 박물관 | 발견 |
| 4 | 강가 | 댐 |
| 5 | 예절 | 공손함 |
| 6 | 수채화 | 미술관 |
| 7 | 자동차 | 전조등 |
| 8 | 언덕 | 바위 |
| 9 | 일 | 정육점 |
| 10 | 도서관 | 서명 |
| 11 | 책 | 저자 |
| 12 | 철로 | 기차 |
| 13 | 에너지 | 기름 |
| 14 | 지구 | 성분 |
| 15 | 결과 | 성취 |
| 16 | 자전거 | 발전기 |
| 17 | 불 | 난로 |
| 18 | 병 | 종이 |
| 19 | 비행기 | 케첩 |
| 20 | 친구 | 신뢰 |
| 21 | 건물 | 오두막 |
| 22 | 산 | 깃발 |
| 23 | 감옥 | 범죄 |
| 24 | 그릴 | 여름 |
| 25 | 산업 | 공장 |
| 26 | 상점 | 인형 |
| 27 | 지하실 | 쇠살대 |
| 28 | 의복 | 덮개 |
| 29 | 신체 | 힙줄 |
| 30 | 위기 | 부족 |
| 31 | 부엌 | 양동이 |
| 32 | 해안 | 사구 |
| 33 | 실험실 | 피펫 |
| 34 | 가게 | 광고 |
| 35 | 풍경 | 습지 |
| 36 | 폭력 | 싸움 |
| 37 | 여자 | 데이트 |
| 38 | 솔기 | 십자수 |
| 39 | 폭풍우 | 대기 |
| 40 | 라디오 | 목소리 |
| 41 | 비 | 통 |
| 42 | 총 | 구경 |
| 43 | 체스 | 루크 |
| 44 | 마제공 | 말굽 |
| 45 | 장난감 | 플라스틱 |
| 46 | 부케 | 튤립 |
| 47 | 극장 | 줄 |
| 48 | 결정 | 통지 |
| 49 | 숲 | 단풍 |
| 50 | 와인 | 꽃 |
| 51 | 결혼식 | 제단 |
| 52 | 전나무 | 나무껍질 |
| 53 | 시계 | 기어 |
| 54 | 겨울 | 사고 |

# 국문초록

## 심층 신경망 및 폐-루프형 자극을 이용한 무구속적 수면 모니터링 및 조절

수면은 우리의 건강을 유지하고 기억력을 향상시키는데 필수적인 역할을 하는 우리 몸과 마음의 자연스러운 상태이다. 수면을 모니터링하고 수면의 질을 향상시키는 효과적인 접근법은 우리의 건강과 행복을 향상 시킬 것이다. 비록 이전의 연구들에서 이를 달성하기 위한 몇 가지 방법들을 제안하였지만, 그 방법들은 구속적이고 실제 환경에서 실용적이지 않으며 장기간 사용하기에는 부적절하다. 따라서, 새로운 접근 방식이 필요하다. 본 학위 논문은 무구속적 심탄도 신호를 이용한 심층 신경망 기반 수면 단계 분류 모델을 제안한다. 또한, 본 학위 논문은 새로운 무구속적 수면 자극 시스템을 제안하고 수면 및 기억력에 미치는 영향을 평가한다.

수면 단계 스코어링은 수면 모니터링의 첫 단계이다. 수면다원검사는 수면을 평가하는 표준 방법이지만, 구속적이고 장기간 수면 모니터링에 사용하기 어렵다. 이러한 한계를 극복하기 위해, 무구속적 방법으로 측정된 심탄도 신호를 이용한 자동 수면 단계 스코어링 장단기 기억 네트워크를 제안한다. 60명 피험자의 심탄도 신호는 PVDF 센서를 사용하여 수면다원검사 동안 기록되었다. 60개의

데이터 중, 30개는 학습용, 10개는 검증용, 20개는 테스트용으로 사용되었다. 심탄도 신호에서 움직임, 호흡, 그리고 심박변이율을 포함한 16개의 파라미터를 추출한 후 정규화하였다. 장단기 기억 신경망 구조에서, 테스트 데이터 세트에 대해 수면 4단계 분류 성능을 평가하였고, 그 결과를 기존 기계 학습 결과와 비교하였다. 수면 4단계 에포크 단위 (30초) 분석은 평균 정확도는 0.74 그리고 평균 코헨의 카파 계수는 0.55를 보였다. 다른 기계 학습 방법 및 이전 연구와 비교했을 때, 제안한 장단기 기억 신경망 모델은 최고 분류 성능을 달성하였다. 심탄도 신호와 함께 장단기 기억 신경망을 사용하면 자동으로 수면 단계를 스코어링 할 수 있으며 가정에서 장기간 수면 모니터링에 사용할 수 있다.

수면의 질을 높이고 수면을 통한 건강 증진을 위해서는 수동적인 수면 모니터링을 넘어서는 수면 조절 방법이 필요하다. 수면 증진을 위한 다양한 자극 시스템이 있지만, 장기간 사용에는 구속적이고 비실용적이다. 본 학위 논문은 새로운 자극 시스템을 제안하고 심장 리듬과 수면에 미치는 영향을 조사함으로써 다른 방법들의 한계를 극복한다. 수면 중 개방-루프 진동 자극의 효과는 수면 마크로구조 및 심박변이율 분석에 의해 평가되었다. 수면 시작 잠복기 파라미터가 유의미하게 감소했지만, 자율신경계 안정화에는 영향을 미치지 않았다. 심장 리듬과 진동 자극 사이의 상호작용을 증가시키기 위해, 새로운 폐-루프형 자극 시스템을 개발하였으며 수면에 적용 가능성을 확인하였다. 10명의 지원자가 약 90분간 낮잠을 자는 평가 실험에

참여하였다. 실험은 하나의 기준 조건과 세 가지 자극 조건으로 구성하였다. 심박변이율과 심박 밀도 분석에서 폐-루프형 자극 방법은 심장 리듬에 영향을 미치고 자율신경계를 안정화시켰다. 작은 디튜닝 퍼센트는 심장 리듬을 더 효과적으로 조절하였다. 청각, 전류, 진동과 같은 수면 자극 방법의 효과를 비교했을 때, 제안한 폐-루프형 자극 시스템이 심장 리듬 조절에 가장 효과적이었다. 심박변이율 분석에서 폐-루프형 자극 방법만이 자율신경계를 안정화시켰다. 따라서 이 시스템은 수면 중에 외부 자극을 적용하는 획기적인 방법이 될 수 있다.

주기적인 외부 자극이 수면과 기억력에 미치는 영향을 조사하기 위해, 밤 수면 동안 폐-루프 진동 자극을 유도하였다. 12명의 지원자가 실험에 참여했으며, 각각 1회의 적응 검사와 자극 조건 및 자극 없음 조건과 같은 두 가지 실험 조건을 수행하였다. 개발된 시스템이 기억력에 미치는 영향은 단어 쌍 학습 과제를 이용하여 평가되었다. 심박변이율 분석 결과 N3 수면 단계 동안 자극 조건에서 부교감 신경 활성도는 유의미하게 증가하였고, 교감 미주 신경 밸런스는 유의미하게 감소하였다. N3 단계의 자극 조건에서 심박수와 자극 사이의 동기화 비율은 유의미하게 증가하였다. 뇌파 스펙트럼 분석은 N3 단계의 자극 조건 동안 저속파 활동 및 세타 주파수 대역에서 향상된 뇌파 스펙트럼 파워를 보였다. 자극 없음 조건과 비교하여 자극 조건에서 기억력 보존이 유의미하게 증가하였다. 이러한 결과는 폐-루프형 자극이 N3 단계의 질과 기억력을 향상 시킨 다는 것을 시사한다. 이 방법은 수면 중 자율신경계 및 신경 기능에 긍정적인 효과가 있다.

제안된 무구속적 수면 단계 분류 방법은 장기간 수면 모니터링에 기여한다. 또한, 제안된 새로운 자극 방법은 수면의 질을 향상시키고 수면 조절을 통해 건강을 향상시킬 수 있는 잠재력을 가지고 있다. 이러한 접근법은 편리하고 안전한 방법으로 수면 모니터링과 향상을 위한 새로운 전략을 열 것으로 기대된다.

---

주요어: 무구속적, 수면 모니터링, 장단기 기억 신경망, 수면 조절, 폐-루프 시스템, 수면의학

학 번: 2014-21547